POLITECNICO DI MILANO

Scuola di Ingegneria Industriale e dell'Informazione

Corso di Laurea Magistrale in Ingegneria Elettrica

GLOBAL MAXIMUM POWER POINT TRACKING METHOD OF PHOTOVOLTAIC SYSTEM UNDER MULTI-PEAK CONDITIONS

Relatore: Prof. Enrico Ragaini

Tesi di Laurea Magistrale di:
Tong Guan
Matr. 533398

Anno Accademico 2017-2018

CONTENTS

LIST OF FIGURES

TABLE OF CONTENTS

SOMMARIO

Con la rapida crescita della domanda di energia e la crescente scarsità di combustibili fossili, lo sviluppo e l'utilizzo delle energie rinnovabili ha ricevuto sempre più attenzione, ad esempio è possibile considerare il notevole sviluppo dei pannelli fotovoltaici. Tuttavia, a causa dell'influenza di diversi fattori incontrollabili, come l'occlusione da parte di uccelli, l'ombra causata dalle nuvole ed altri fattori interni ed esterni, si registrano nella pratica dei valori differenti rispetto a quelli previsti dalla teoria. In particolare la curva di uscita del modulo fotovoltaico presenta più punti di picco. Pertanto, lo studio del metodo di tracciamento del punto di massima potenza globale di un pannello fotovoltaico in presenza di più picchi è di grande importanza, in quanto permette ai moduli fotovoltaici di erogare la massima potenza.

Questa tesi presenta inizialmente uno studio comportante il rilevamento del punto di massima potenza globale in condizioni di più picchi. In primo luogo, è proposta una Metodo di Ricottura "Simulated Annaeling Method" (SA) e dell'Ottimizzazione dello Sciame di Particelle "Particle Swarm Optimization" (PSO), che permettono di individuare il punto di massimo globale. Questo algoritmo combina il vantaggio di convergenza asintotica dell'algoritmo SA e il vantaggio della diversità dei gruppi presente nell'algoritmo PSO. Come risultato questa tecnica può mantenere l'equilibrio tra ricerca globale e ricerca locale. Per garantire l'accuratezza ed una rapida convergenza, la simulazione è ripetuta 50 volte e la deviazione è ottenuta confrontando il tempo di convergenza effettivo con quello atteso.

In secondo luogo, analizzando le prestazioni dell'algoritmo, è possibile studiare ogni parametro ed ottenere l'influenza di ciascun parametro sull'algoritmo. Allo stesso tempo, questa tesi presenta un grafico della tendenza relativa al cambiamento dei parametri attraverso gli esperimenti statistici, e fornisce i parametri tali per cui le prestazioni generali dell'algoritmo siano ottimali.

Infine, questa tesi convalida l'algoritmo SA + PSO attraverso esperimenti hardware. Per effettuare questa operazione è prima necessario configurare la piattaforma sperimentale hardware nella sua completezza. Gli esperimenti sono eseguiti in condizioni di picco singolo e multiplo, tali da verificare l'efficacia dell'algoritmo nell'individuare il punto di massima potenza globale. I risultati sperimentali dell'hardware confermano la validità dell'algoritmo proposto nell'applicazione pratica.

ABSTRACT

With the rapid growth of energy demand and the increasing scarcity of fossil fuels, the development and utilization of renewable energy has received more and more attention, such as solar energy. However, due to the influence of some uncontrollable factors, such as bird occlusion, cloud shading and other external and internal factors, all these factors lead to mismatched photovoltaic components. The mismatch phenomenon causes the output curve of the PV module appear multiple peak points. Therefore, the study of the global maximum power point tracking method of a photovoltaic panel under multi-peak conditions is of great significance for photovoltaic modules to achieve the maximum power output.

This thesis begins with tracking global maximum power point under multi-peak conditions. Firstly, this thesis proposes a simulated Annealing method (SA) and Particle Swarm Optimization (PSO) mixed global maximum power point tracking method. This algorithm combines the asymptotic convergence advantage of SA algorithm and the group diversity advantage of PSO algorithm. It can keep the balance between global search and local search. In order to ensure the accuracy and fast convergence, we do experiment 50 times and get the deviation comparing convergence time with the expected.

Secondly, when we analyze the performance of the algorithm, we may summarize each parameter in the algorithm and obtain the influence of each parameter on the algorithm. At the same time, this thesis presents a trend graph of parameter changing through statistical experiments, and gives the improved optimal parameters so that the overall performance of the algorithm is optimal.

Finally, this thesis validates SA+PSO algorithm again through hardware experiments. The hardware experimental platform is set up completely. We do experiments under the single-peak and multi-peak conditions to verify the algorithm that can track the global maximum power point. The hardware experimental results validate the implement ability of the proposed algorithm in practical application.

1 INTRODUCTION

1.1 Research Background and Significance

Electric energy is a secondary energy. It can be converted from oil, coal or other new energy sources. According to some statistics and predictions, fossil fuel energy is still the most used fuel energy in the world; however, the proportion of coal energy is gradually decreasing [1]. And as the number of world population is increasing, the traditional fossil energy consumption will be larger. It is understood that oil energy reserves in the world are sufficient for up to 50 years, and coal energy reserves in the world can be used for up to 114 years [2]. At present, the energy crisis has become more and more worthy of attention, and it has become a serious problem that the world has to face and solve.

In addition, people began to pay attention to environmental protection. From the global warming trend of previous years to the frequent fog and haze weather in recent years, these have been driving people to find new types of clean energy and improve them. From this trend, at the moment the use of low-carbon economic growth models is more important, and this model has gradually replaced the use of high-carbon traditional fossil energy economic growth model [3].

At the same time, from the perspective of Chinese electricity consumption, China National Energy Administration announced in 2017 that total social power consumption was 6307.7 billion kwh, an increase of 6.6% year-on-year, an increase of 1.6 percentage points from the same period last year [4]. In 2017, the country's newly added power production capacity (formally put into operation) was 137.27 million kilowatts, an increase of 6.5% year-on-year. Among them, hydropower is 12.87 million kilowatts, power generation amount increased by 1.7% year-on-year; thermal power is 45.78 million kilowatts, power generation amount increased by 5.2% year-on-year [5]. The power generation amount of clean energy grew by 10% year-on-year, and the growth rate was 4.8 percentage points higher than thermal power. Among them, hydropower, nuclear power, wind power and solar power generation amount increased respectively by 1.7%, 16.5%, 26.3%, and 75.4% year-on-year[6]. This can be

illustrated that the power generation proportion of clean energy in China is increasing, especially solar energy, which means that the growth of power generated by photovoltaic energy is extremely fast.

From China's policies, the state has vigorously supported new energy sources and reduced the abandonment of water, winds, and light energy. China's trans-provincial trans-regional electricity market trading have effectively reduced abandoned winds and abandoned light phenomenon. According to preliminary statistics, trans-provincial clean energy delivered 588.7 billion kwh of electricity, which accounted for 54.5% of the total electricity delivered. Southwest hydropower delivered 263.8 billion kwh, an increase of 10.2%, which played a positive role in reducing water and electricity in Southwest China. Achieving wind power and photovoltaic power generation trans-provincial-to-provincialized transaction power of 36.6 billion kwh, an increase of 26% year-on-year [7], alleviating the pressure of abandoning wind and deserting the "Three Norths" region.

Summarizing the analysis of light energy above, the following points are drawn: First, solar energy is clean energy without pollution. During the photoelectric conversion process, no SO2, dust, fine particles, etc. that pollute the air are generated; Inexhaustible, the amount of energy radiated to the earth's surface each year is roughly 130 trillion tons if converted into coal [8]. This reserve is inexhaustible for human beings. Again, from our country's policy, The government's subsidies for photovoltaic power have increased steadily, especially for companies such as Goldwind Co. ted and Envision Co. ted that have invested heavily in new energy photovoltaics, and universities and companies are strongly encouraged to study the efficiency of photovoltaic power generation; Finally, the global 2017 photovoltaic installation The total amount reaches 300GW. Among them, China led the global market with 34.54GW, accounting for 11.51% of the total installed capacity in the world, while the United States and Japan respectively reached 14.76GW and 10.5GW[9]. It should be noted that the installed capacity of photovoltaic power generation in China accounted for only 1.2% [10] in 2016, indicating that the growth momentum of this ratio is very strong and the potential for future development is huge. In general, all the above conditions are driving the development of photovoltaic power generation. In the future, new energy sources with solar energy as the core power will be the dominant power generation method.

The current photovoltaic power generation process is dependent on the environment and the energy obtained through solar energy conversion is unstable. It is affected by factors easily

such as light irradiance, load changes, temperature changes, weather, etc. These factors will directly lead to the output power of photovoltaic panels. Changes have seriously affected the photoelectric conversion efficiency of photovoltaic panels. The primary reason for the low efficiency of photoelectric conversion is material issues, followed by control algorithm problems. For photovoltaic cell materials, if you want to improve it must invest a lot of manpower, material resources and time, but the effect of improvement may not be obvious. Therefore, optimizing the Maximum Power Point Tracking (MPPT) in photovoltaic power generation systems is the best way to increase the photoelectric conversion efficiency of solar cells.

1.2 The Advantages and Disadvantages of PV Power Generation

Photovoltaic industry characterized by solar cells has been recognized as one of the major renewable energy sources in the future, due to its unlimited reserves, universal existence, cleanliness of use, and practical economy. As shown in Table 1-1 below, this thesis lists several advantages of photovoltaic power generation.

Table 1-1 Advantages of Photovoltaic Power Generation

Direct use of solar energy	Large reserves, clean energy Everywhere
Photoelectric conversion directly	Simple structure, no moving parts, easy to use, unmanned management Manufacturing requires low energy consumption, as long as 2-3 years to recover the investment Can be used as building materials instead of roofs and windows
Distributed power generation system	No power supply and power transmission equipment After networking, there is a flat peak effect on urban electricity.

In addition, the cost of photovoltaic power generation is continuously declining, which provides a good opportunity for a large number of photovoltaic power generation applications. China National Development and Reform Commission recently issued a notice on the on-grid tariff policy for photovoltaic power generation. The nationwide PV power plant project implements the on-grid tariffs of 1 RMB/kwh and 1.5 RMB/kwh [8]. The promulgation of this electricity price policy has undoubtedly become an important driving force for accelerating the scale of photovoltaic power generation applications. The

promulgation of 1 yuan benchmark price policy will surely open up a new situation in the photovoltaic market.

Although photovoltaic power generation has above advantages, the biggest problem that troubles photovoltaic power generation is efficiency. In order to realize higher power generation efficiency of the PV system, techniques such as improving the photoelectric conversion efficiency, increasing the effective acceptance area of the photovoltaic panel, and the global maximum power point tracking technology may be used. Photoelectric conversion efficiency of crystalline silicon photovoltaic cells which accounts for the largest market is relatively low, the conversion efficiency is no more than 20%. However, the photoelectric conversion efficiency belongs to the physical field, not within the scope of this thesis. Therefore, the efficiency of the photovoltaic system is more dependent on the control of the maximum power point tracking technology.

This thesis focuses on the global maximum power point tracking technology to improve the overall output efficiency of photovoltaic panels. However, in the case of partial shadow shading, the power-voltage (PV) curve of the PV array presents multiple peak points, which poses a great challenge to the traditional MPPT algorithm. The traditional MPPT algorithm is easily trapped in the local maximum power point rather than the global maximum power point. Therefore, using an effective MPPT algorithm under multi-peak conditions enables the photovoltaic system to operate at the global maximum power point regardless of whether there is partial shielding or not, which can greatly improve the overall efficiency of the photovoltaic system.

1.3 Multi-peak Phenomenon of Photovoltaic System

The solar cell is mainly a photoelectric conversion between solar energy and electric energy. This conversion requires solar panel devices with different specifications. Solar cells can be connected in series or parallel to form photovoltaic modules. Photovoltaic modules can be connected in series or parallel to form photovoltaic arrays. No mismatch occurs under ideal conditions, the overall output characteristics of the photovoltaic system are similar to the output characteristics of a single photovoltaic panel. There is only one maximum power point on the power-voltage characteristic curve. The traditional MPPT methods such as Perturb & Observation (P&O) [3] or Increment Conductance (INC) [4] can track the maximum power point.

However, due to the differences in the angles of placement, shadowing of surrounding objects and dust cover and so on, the light and temperature are uneven and the aging degree is different between the photovoltaic panels during the actual production process. Mismatch problem [6] will occur during the production process of the factory so that it leads to multiple peaks in the overall power-voltage output characteristic of the PV system, as shown in Figure 1-1(b). At this moment, traditional MPPT method can easily fall into local maximum power point instead of global maximum power point. In this way, the output power is much less than the achievable global maximum power. This will result in a significant reduction in the utilization of the photovoltaic system, reduce the conversion rate of solar energy and seriously affect economic efficiency. The output power of the PV array is less than the sum of the power of each PV module, and the output power of the PV modules is less than the sum of the power of each PV cell. This intermediate power loss is called multi-peak loss. Obtaining maximum energy conversion efficiency requires that the photovoltaic panel must be operated at the global maximum power point. Therefore, tracking the global maximum power point becomes the key to solve this shadowing problem.

We take the photovoltaic string which composed of three photovoltaic panels in series as an example. Because the shading is blocked or the orientation is different, the three photovoltaic panels are operated under different irradiance conditions, as shown in Figure 1-1(a). The irradiance difference results in inconsistent output characteristics of the three photovoltaic panels. The current-voltage curve of the entire photovoltaic string appears multiple poles. The power-voltage curve appears the characteristics of multiple local maximum power points (LMPP).

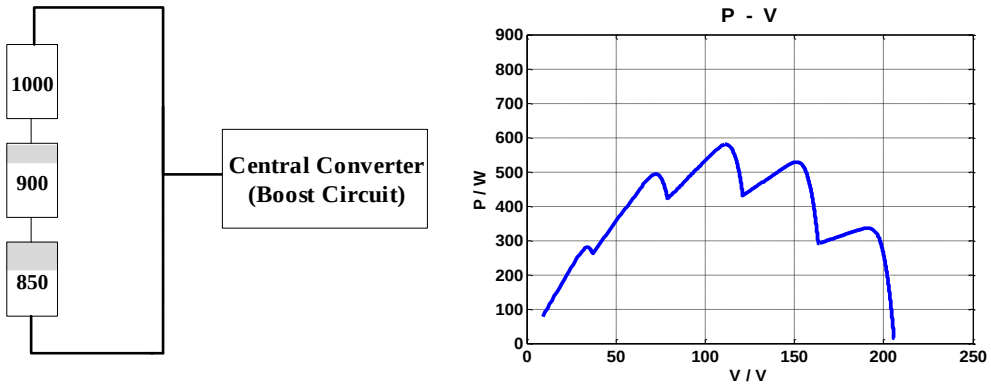

(a) Three photovoltaic panels with different light intensities

(b) Multi-peak power-voltage output characteristics

Figure 1-1 P-V output characteristics of a PV system in case of multi-peak conditions

If a PV module is partially shaded or unevenly illuminated, hot spots phenomenon will occur which causes serious multi-peak loss problems. PV arrays will also have multi-peak problems when the irradiance is uneven. If one of the PV cells with ageing problems or load mismatch problems, the associated photovoltaic components and multi-peak problem will occur. The multi-peak problem brings many negative effects which leads to multiple peaks in the PV characteristic curve. The PV array or PV module cannot work at the point of maximum conversion efficiency, and even the PV array cannot work normally and the PV array device will be damaged. Multi-peak problem is common in photovoltaic power generation systems and their dangers cannot be underestimated. On the one hand, the output multi-peak characteristics of the PV array may cause traditional maximum power point tracking method invalidate. It will cause the system operating at the local maximum power point and unable to output the maximum power, then the system may oscillate around multiple local maximum power points.[5] Therefore, it will lead to the oscillation of the output power which directly affects the stability of the grid-connected system. On the other hand, because the existing control strategy cannot make each PV module operate at each maximum power point under mismatch conditions, the total output power of the PV modules after series and parallel connection is often less than the maximum output power of each PV module. These problems will cause a non-negligible energy loss. Therefore, the significance of studying the multi-peak problem lies in minimizing the power loss caused by the multi-peak problem, ensuring that the photovoltaic array or photovoltaic module operates at the maximum conversion efficiency power point. Thus, the utilization of the photovoltaic system is optimized. So far, scholars have not studied the multi-peak problem very deeply. The research direction almost analyzes the mismatch problem. The current solution for the multi-peak problem is the Global Maximum Power Point Tracking (GMPPT) algorithm.

1.4 Research Status at Internal and Abroad

There are many reasons why Chinese solar manufacturers are experiencing bottlenecks. In the past, Europe was the core of photovoltaic power generation in the world. Therefore, China's solar energy relied on the European market heavily. More than 90% of China's solar cells exported to Europe and affected by the euro easily. For example, Chinese production capacity was about 2.4 million kilowatts in 2009. However, China's installed capacity was only 120,000, which exceeded the export percentage of 90%. European countries as an

important export country of China, including Spain and Italy, Germany, the Czech Republic and so on, new installed capacity exceeds 4.2 million kilowatts which accounts for more than three-fifths of the world [10]. The euro-zone debt storm that broke out in 2009 caused euro to fall. It caused Chinese photovoltaic cell manufacturers to suffer a large area damage. These bad factors indicate that Chinese manufacturers have a great crisis. In order to cope with this factor, they try to reduce costs and increase demand to control the risks.

The global maximum power point tracking method can find the global maximum power point of the photovoltaic array under various multi-peak conditions so that the photovoltaic array outputs its maximum power. In recent years, scholars have studied the effect on photovoltaic output characteristics based on different MPPT algorithms in photovoltaic modules. Different MPPT algorithms have different effects on the output power of photovoltaic modules. The ultimate goal is to find a more stable and efficient MPPT algorithm. At present, the traditional methods to track the global maximum power point are: perturbation observation method (P&O) and conductance increment method (INC). Perturbation observation method is relatively simple to implement in principle, so scholars study more. However, in a stable state the operating points of the disturbance observation method often fluctuate near the global maximum power point, resulting in power loss problems. Moreover, the disturbance observation method cannot be applied when the irradiance changes rapidly. Based on this problem, domestic and foreign scholars have also made some improvements. An improved perturbation observation method is also proposed [7], which is also called the POC (Perturb Observe and Check) algorithm. This algorithm uses perturbation observation method when searching local peaks, and adopts a fast scanning mechanism so that it can reduce the search time in the non-maximum power point region effectively. The reference [8] estimated the possible local maximum power point interval according to the parameters of the PV array, then used the conventional MPPT algorithm to accurately track the LMPP in this interval. Finally, the LMPPs in each interval were compared; the largest power is the GMPP (Global Maximum Power Point, GMPP). The reference [9] studied an MPPT algorithm based on complex-valued functions. The function consists of a two-dimensional Gaussian function and an arctangent function. This function is used to determine the duty cycle of the DC-DC converter in the PV system. This can make the PV system operate in GMPP under any environment and load conditions. The reference [10] proposed a mixed evolutionary algorithm based on the combination of differential

evolution algorithm and Particle Swarm Optimation (PSO) algorithm. This algorithm can detect the global maximum power of photovoltaic system under partial shading condition.

At present, the methods of tracking the global maximum power point using artificial intelligence methods include: fuzzy control method, BP neural algorithm, particle swarm optimization algorithm, simulated annealing algorithm and so on. The reference [11] introduced an artificial bee colony algorithm to cope with the uneven irradiance. The reference [12] researched a MPPT algorithm based on simulated annealing (SA) and analyzed the influence of various parameters on the algorithm performance. An enhanced SA algorithm is proposed in the reference [13]. A two-stage MPPT algorithm is proposed in the reference [14]. The first-level algorithm first detects if there is shadow occlusion, and the second-level algorithm tracks the GMPP based on the slope change of the duty cycle and continuous sampling of the PV array power-voltage curve. The reference [15] proposed a research based on the SA+PSO mixed algorithm for NMPC. Considering the research in this thesis, the SA+PSO mixed algorithm can also be used to GMPPT. At present, there are a large number of existing GMPPT algorithms with different methods. Their classification and comparison will be described in detail in Chapter 2.

Although the conventional global maximum power point tracking method can track the global maximum power point under multi-peak conditions, the tracking speed is slow and the tracking time is long. The advantage of the artificial intelligence method in tracking global maximum power points under multi-peak conditions is even more obvious. The particle swarm optimization and simulated annealing artificial intelligence algorithms are optimal in the tracking accuracy and tracking speed respectively. Therefore, this thesis proposes a GMPPT algorithm based on SA+PSO mixed method. This proposed algorithm will be deeply researched and verified by experimental simulation.

1.5 The Main Research Content of This Thesis

This thesis proposes a new global maximum power point tracking method based on mixed simulated annealing and particle swarm optimization. Compared with the existing particle swarm optimization and simulated annealing method, the proposed algorithm combines the advantages of the two methods and does not cause more complexity. It can not only jump

out of the local maximum power point, but also can accurately track the global maximum power point.

The main work and structure of this thesis are as follows:

Firstly, this thesis elaborated on photovoltaic cells and specific MPPT technologies, and briefly explained how to deal with photovoltaic arrays under partial shading condition. According to the characteristics of the photovoltaic cell, this thesis set up a physical model of the photovoltaic cell. Then this thesis considered the influence of the outside temperature and solar irradiance on the photovoltaic array, and derived its external characteristics. In order to analyze the effect of partial shadowing of photovoltaic cells, this thesis analyzes the relevant parameters affecting its performance and uses Chrome software to emulate the characteristics of photovoltaic cells. Then the software obtains the P-V curve of the photovoltaic cells at that moment.

Secondly, for the partial shading condition, this thesis analyzes the causes of the multi-peak condition in the photovoltaic system, gives the research direction of the global maximum power point tracking method. Then this thesis distinguishes various types of algorithms and summarizes the working principles of several common algorithms. This thesis emphasizes the working principle of the MPPT algorithm of the existing particle swarm optimization algorithm and simulated annealing method. Thus this thesis proposes a mixed algorithm based on SA+PSO to solve the multi-peak problem. It presents the working principle of the SA+PSO mixed algorithm in details and calculates the relevant parameters. This thesis summarizes the advantages of the mixed algorithm from tracking accuracy and tracking speed two aspects.

Thirdly, this thesis uses Matlab/Simulink software to verify the SA+PSO mixed global maximum power point tracking method results. We use SA+PSO mixed algorithm to track GMPP under single-peak and multi-peak conditions. Multiple parameters in the SA+PSO mixed algorithm are analyzed one by one. Then this thesis summarizes the trend of the parameters affecting the output power of the photovoltaic panels. In order to verify the robustness of the SA+PSO mixed algorithm, the thesis summarizes the results of the tracking time and the tracking accuracy in 50 iterations. The proposed SA+PSO mixed algorithm is compared with the existing SA and ESA algorithms to verify the superiority.

Fourth, in order to verify that the algorithm can be implemented in hardware, this thesis used DC-DC Boost circuit for hardware experiments. The experiment is divided into single-peak and multi-peak conditions. The output power value of PV array and the time to reach the maximum power are obtained through an oscilloscope. This is the same as the expected maximum power point obtained from the characteristic curve in the photovoltaic panel. Now the proposed SA+PSO algorithm can be well verified.

Finally, this thesis summarizes the proposed SA+PSO algorithm and draw conclusions, then look forward to the future work.

2 PV ARRAY COMPOSITION PRINCIPLE AND EXISTING ALGORITHM RESEARCH

This chapter first introduces the equivalent model and composition principle of PV arrays, then analyzes the causes of partial shading and multiple peaks condition. In the last, this chapter detects the output characteristics of PV arrays under multi-peak conditions. It requires global maximum power point tracking method when solving the multi-peak problem. GMPPT algorithms are divided into conventional algorithms and artificial intelligence algorithms. The artificial intelligence algorithm has been developed rapidly in recent years. Among them, the performances of the Particle Swarm Optimization algorithm and simulated annealing are better. This thesis compares several existing GMPPT algorithms, and then gives the best choices in existing algorithms from the tracking time and the tracking accuracy aspects.

2.1 Principle Composition and Equivalent Model of PV Array

Photovoltaic energy conversion devices are solar cells, also called photovoltaic cells. The principle is the photovoltaic effect. When sunlight or other light hits the solar cell, the cell absorbs light energy and creates a photoelectron-hole pair. Under the action of the battery's built-in electric field, photoelectrons and holes are separated. The accumulation of different charges at both ends of the battery produces a “photovoltaic voltage”, which is the “photovoltaic effect” [16]. If the electrodes are drawn on both sides of the built-in electric field and the load is connected, the load will have a “photo-generated current” flowing to obtain the power output. In this way, the sunlight energy is converted into electricity directly. When a plurality of photovoltaic cell modules are connected in series to form a photovoltaic array, the total output power is equal to the sum of the output powers of the respective cell assemblies. Photovoltaic cells are made of monocrystalline silicon and convert solar energy

into electrical energy according to the photovoltaic effect. After the load is connected to the circuit, it will have an output current.

The operating principle of a solar cell is as follows: The atom of a substance is composed of a nucleus and an electron. The nucleus is charged positively and the electron is charged negatively. In the absence of external interference, electrons rotate around the nucleus [17]. There are four electrons around the silicon atom's nucleus. When there is a certain light irradiance, the electrons will absorb the photon energy and leave the nucleus. Thus, it will generate an electron-hole pair. When different impurities are incorporated into the silicon crystal, a P-type semiconductor and an N-type semiconductor are obtained respectively. When these two are combined, a P-N junction is formed at the interface, thereby generate a barrier electric field. Under the action of the barrier electric field, electrons are transferred to the direction of the N-type semiconductor, and holes are transferred to the direction of the P-type semiconductor. Thus, an electric field in the opposite direction to the potential of the barrier electric field is generated. After a part of barrier electric field is cancelled, the P-type semiconductor is positively charged, the N-type semiconductor is negatively charged, resulting in a photovoltaic electromotive force. After the load is connected, a current output power is generated.

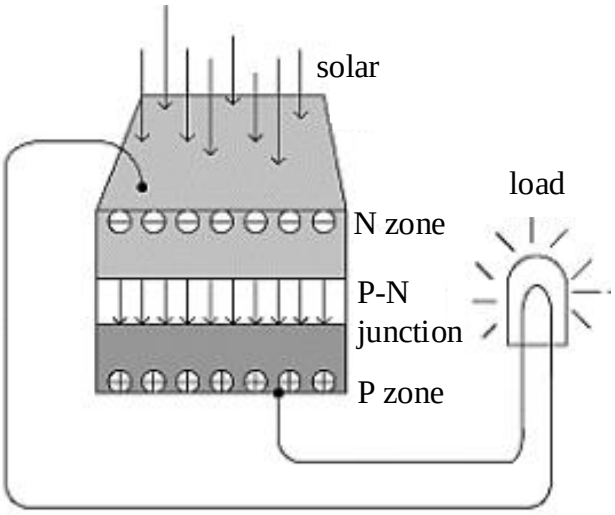

Figure 2-1 Photovoltaic effect schematic diagram

According to the description of the photovoltaic effect, the sunlight can be divided into three parts, one is the light energy used by the solar cell, in this part the photon is absorbed by the solar P-N junction; the remaining two parts are the unusable light energy. It includes the

light energy reflected by the photovoltaic cell and the light energy absorbed by the PN junction by other parts of the photovoltaic cell. Therefore, this also become one of the reasons why the photovoltaic cell utilizes low solar energy efficiency.

The equivalent circuit of a photovoltaic cell is shown in Figure 2-2. The two important parameters that describe the characteristics of a photovoltaic cell are:

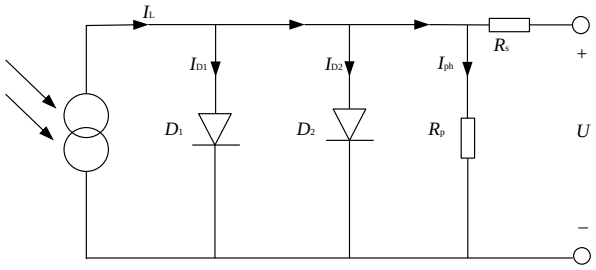

Figure 2-2 Photovoltaic cell equivalent model

First, short-circuit current I_{sc}, the short-circuit current is related to the area of the photovoltaic cell, the short-circuit current of one square centimeter photovoltaic cell is about 16-30 mA, and is proportional to the incident spectral irradiance.

Second, no-load voltage U_{oc}, no-load voltage is proportional to the logarithm of the incident spectral irradiance, and no relation with the area of the photovoltaic cell. Assuming 100 MW of sunlight per cm2, the no-load voltage is about 450-600 mV, and the maximum is 690 mV.

Generally, we think that the current of the current cell is proportional to the light irradiance, the parallel resistance R_p represents the leakage resistance of the photovoltaic cell, and R_s is used to represent the series resistance of the actual photovoltaic cell. The figure is the most common battery model, the advantages are simple and conducive to analysis, the formula is as follows:

$$I_L = I_{ph} - I_d - I_{sh} \qquad (2\text{-}1)$$

Among them, I_{ph} is photocurrent; its value is proportional to the area of the photovoltaic cell and the irradiance of the incident light. I_d is a dark current, which refers to the unidirectional current flowing in the P-N junction under the action of external voltage when there is no light. T is thermodynamic temperature. R_S and R_{SH} are inherent resistances of photovoltaic cells. Because R_S is small and R_{SH} is large, so they are negligible for ideal calculations.

$$I_{\mathrm{d1}} = I_{01}\left(e^{\frac{q(V+IR_S)}{AKT}} - 1\right) \quad (2\text{-}2)$$

$$I_{\mathrm{d2}} = I_{02}\left(e^{\frac{q(V+IR_S)}{2KT}} - 1\right) \quad (2\text{-}3)$$

I_{01} is the reverse saturation current of the photovoltaic cell diode d_1 and the diode d_2, q is the electron charge, K is the Boltzmann constant, A is the quality factor of the diode 1, and the quality factor of the d_2 is assumed to be A= 2, so the photovoltaic cell output I-V equation is:

$$I_{\mathrm{L}} = I_{\mathrm{ph}} - I_{01}\left(e^{\frac{q(V+IR_S)}{AKT}} - 1\right) - I_{02}\left(e^{\frac{q(V+IR_S)}{2KT}} - 1\right) - \frac{V+IR_S}{R_{sh}} \quad (2\text{-}4)$$

$$U_{\mathrm{oc}} = \frac{AKT}{q}\ln\left(\frac{I_{\mathrm{sc}}}{I_0} + 1\right) \quad (2\text{-}5)$$

The expression of the open-circuit voltage U_{oc} is as follows:

$$U_{\mathrm{oc}} \approx A \times U_T \times ln\left(\frac{I_{\mathrm{sc}} - {U_{\mathrm{oc}}}/{R_{\mathrm{sh}}}}{I_0} + 1\right) \approx\times U_{\mathrm{T}} \times ln\left(\frac{I_{\mathrm{sc}}}{I_0}\right) \quad (2\text{-}6)$$

Among them, A is the ideal factor.

2.2 Analysis of PV Panels under Multi-peak Conditions

2.2.1 Causes of Partial Shadows

For photovoltaic power generation systems, shading is the most common and complex condition. As shown in Figure 2-3, photovoltaic arrays are installed on roofs or other building structures generally. Because there are obstacles such as trees, power poles, and cable lines around buildings, so when the light angle changes with the season and time. The above obstacles may have a partial shadow on the PV array.

Figure 2-3 Modular structure of PV system

In addition, a similar situation can occur when there is dirt on the photovoltaic array or when some of the battery elements are damaged. Because some houses are herringbone roofs, the modules will have different orientations or incident angles when installed, which will cause imbalance light, as shown in Figure 2-4.

Figure 2-4 Partial shadow conditions on photovoltaic panels

For large-scale photovoltaic power generation systems, large areas of cloud cover and dirt are the main causes of uneven light. For space solar power stations, shading conditions are also common. Since the solar panels in the space cannot dissipate heat, if there is a hot spot effect, the consequences are serious. Therefore, the method of closing the shaded module is used to prevent the hot spot effect generally.

For portable, mobile solar equipment, such as solar cars, handheld solar equipment, etc., due to the equipment being in the process of moving, it will produce shadows. Other mismatch phenomena, such as the differences in the factory specifications of PV modules, the slicing problems in the assembly process (splitting problems are particularly common among many domestic solar manufacturers), and the differences in the temperatures of various solar energy solar panels are all array mismatch phenomenon.

2.2.2 Multi-peak Condition and Solution

Photovoltaic panel shading problems will cause the multiple peaks of photovoltaic system's output characteristic curve. In the entire photovoltaic power generation system, there are many control algorithms, such as battery charge and discharge control algorithm, photovoltaic array MPPT algorithm, the components gating algorithm and the inverter control algorithm of inverter topology. Among the most directly related, the greatest impact on the efficiency of solar energy conversion is the photovoltaic array MPPT algorithm.

The basic principle of MPPT is explained by the impedance equivalent theory in the following given in the circuit principle:

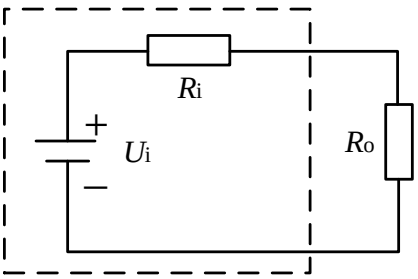

Figure 2-5 linear circuit diagram

Figure 2-6 is a simple linear circuit diagram. U_i is the ideal voltage source, R_i is the equivalent internal resistance of the power supply, and R_o is the external resistance of the circuit. The power consumed in the external resistor is calculated by Equation 2-7:

$$P_{R_o} = I^2 R_o = \left(\frac{U_i}{R_i + R_o}\right)^2 R_o \tag{2-7}$$

R_o for derivation:

$$\frac{dP_{R_i}}{dR_o} = U_i^2 \frac{R_i - R_o}{(R_i + R_o)^3} \tag{2-8}$$

Let the derivative is equal to zero, that is:

$$\frac{dP_{R_i}}{dR_o} = U_i^2 \frac{R_i - R_o}{(R_i + R_o)^3} = 0 \tag{2-9}$$

After compilation, get formula 2-10:

$$R_o = R_i \tag{2-10}$$

That is, when the circuit external resistance is equal to the internal resistance, the external resistor consumes the most energy.

In the linear circuit shown in Figure 2-5, to maximize the power consumed by the external resistors, set the internal resistance equal to the external resistance. According to the

introduction of the photovoltaic cell in the previous chapter, the internal resistance of the photovoltaic cell is not fixed, and its value changes with the external environmental conditions. If the external resistance is still set according to the above method, the photovoltaic cell is not considered. The nonlinear change of the internal resistance makes it difficult to achieve real-time control of the maximum power output of the photovoltaic cell.

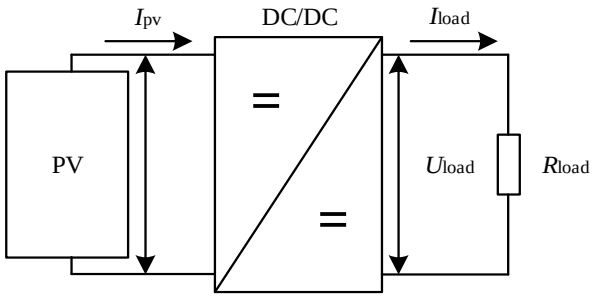

Figure 2-6 Schematic diagram of MPPT algorithm in photovoltaic system

In order to change in the external environment, the photovoltaic cell always outputs the maximum power to achieve real-time control of maximum power point tracking. A conversion circuit is usually connected in series between the photovoltaic cell and the load, as shown in Figure 2-6, where the conversion circuit is considered as an external load connected to the photovoltaic cell. When changing the duty cycle of the conversion circuit, the equivalent resistance of the circuit also changes. Therefore, when the external environmental conditions of the photovoltaic cell change, the duty cycle of the circuit can change through technology, so that the equivalent resistance of the external circuit is equal to the internal resistance of the photovoltaic cell, and the internal and external resistance of the photovoltaic power generation system can be achieved under any conditions. Matching to achieve real-time control of the maximum output power of photovoltaic cells.

MPPT algorithm adjusts the operating status of the electrical module (voltage or current) when the external light conditions such as light irradiance or temperature or partial shaded photovoltaic array change, and keeps the output power of the PV array at the maximum value under current conditions. . Without the control of the MPPT algorithm, the output energy utilization of the PV array will become lower. If there is a partial shadow blocking the PV array, use an improper MPPT algorithm, such as the traditional maximum power point tracking method will fail at multi-peaks condition. Therefore, how to find the global maximum power point on the multi-peak power-voltage curve quickly and accurately is a problem that must be solved. The occlusion phenomenon also causes serious power

mismatch, slow convergence of the algorithm, poor tracking accuracy, etc., making it impossible for the PV array to capture the maximum power value in real time, thereby reducing the power generation efficiency of the entire system.

2.3 Detection of PV Array Output Characteristics under Multi-peak Conditions

It can be known that from the output characteristic equation of photovoltaic cells, the parameters of the physical model determine the output characteristics of the photovoltaic cell jointly. Changes in the model parameters will directly affect the output characteristics of the photovoltaic cell. Photovoltaic module output characteristics test platform is shown in Figure 2-7.

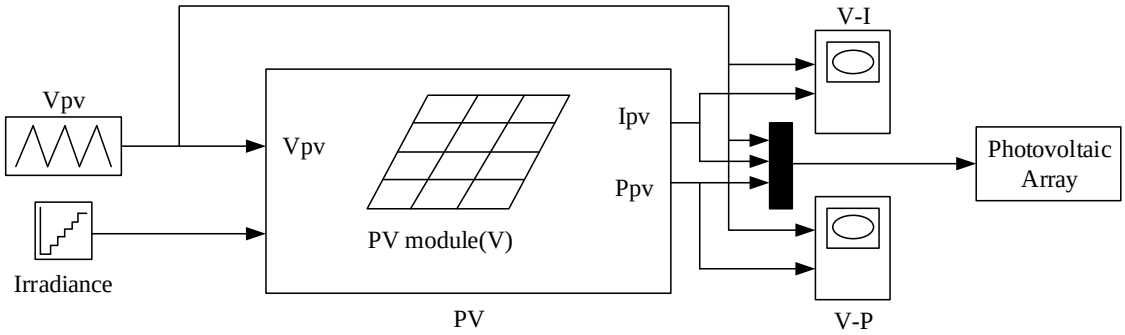

Figure 2-7 Photovoltaic cell module output characteristics test platform

The output characteristics of solar photovoltaic modules are affected by many factors, which temperature and light irradiance are the two main influencing factors. The power-voltage, current-voltage characteristics of solar photovoltaic cells can be detected by the test platform.

PV module parameters are shown in Table 2-1 below:

Table 2-1 PV module parameters 1000W/m^2,25°C

PV module research parameters	Value
Open circuit voltage	11V
Short circuit current	4.7A
Rated current	4.44A
Rated voltage	9V
Number of bypass diodes	1
Rated power	40W

The table of irradiance changes in PV module is shown in Table 2-2 below:

Table 2-2 Photovoltaic module light irradiance

case	Irradiance W/m^2			
	S_1	S_2	S_3	S_4
1	1000	1000	1000	1000
2	900	900	900	900
3	700	700	700	700
4	500	500	500	500
5	700	800	900	1000
6	500	600	800	1000
7	350	600	800	1000
8	150	300	700	1000
9	220	360	640	850

A total of four experiments were done in this thesis, as shown in Figure 2-8 below. Figure 2-8(a) shows the current-voltage characteristics when the temperature is constant and the uniform light irradiance changes. Figure 2-8(b) shows the power-voltage characteristics when the uniform light irradiance changes (case 1-case4 in Table 2-2). For 1000W/m^2 in case 1, the MPP voltage is the rated voltage of the string. As the light irradiance decreases, the output power of the photovoltaic panel decreases due to the drop of the current I_{PV} and the voltage $V_{PV.}$ When the light irradiance increases, the output power of the photovoltaic panel also increases. The short-circuit current is mainly affected by the radiation level, and the open-circuit voltage is mainly affected by the temperature. However, the change interval of the open-circuit voltage is only within a very small range. Therefore, the most important factor affecting the output power of the solar photovoltaic cell is light irradiance.

Fig. 2-8(c) is the current-voltage characteristic curve when the light irradiance changes under the condition of constant temperature and multi-peak. Fig. 2-8(d) is the power-voltage characteristic curve when the light irradiance is unchanged and the temperature changes (Case4 - case6). In case 6, there are four peaks in the P-V characteristic. The first peak (the rightmost peak) is the GMPP (83.47 W) that occurs at 36.35 V. For this case, it is observed that the first peak appeared to the right of the array's rated voltage (33.95 V). In case 8, the third peak is 50.51W of GMPP, which appears at 16.04V. The first peak (2.02W) occurs at 37.17V and its voltage is greater than that under uniform irradiation again. Therefore, under the uniform light irradiance, the first peak voltage under partial shadow will be located on the right side of the MPP voltage, while the MPP current will decrease. It can be concluded from the figure that when the temperature is constant and the light irradiance increases, the

open circuit voltage of the solar photovoltaic panel remains basically unchanged and only floats within a relatively small range, while the short-circuit current changes greatly, and it increases with the radiation level increase.

From the above analysis, it can be seen that changes in the irradiance and temperature all affect the output characteristics of the photovoltaic cell, resulting in a decrease in the photoelectric conversion efficiency of the cell and a non-linear output characteristic curve. In order to let photovoltaic panel always output maximum power at different irradiances and temperatures, maximum power point tracking method is required.

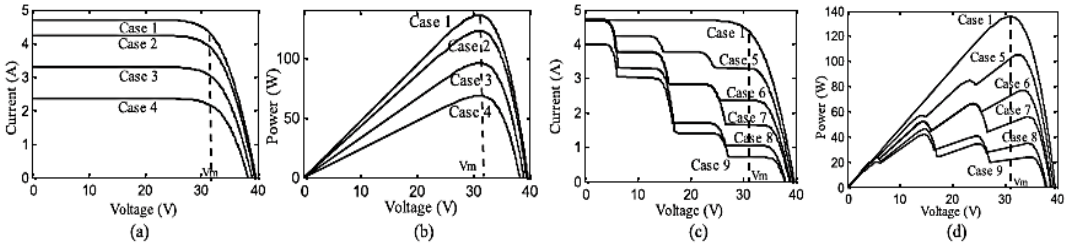

Figure 2-8 I-V Characteristic Curve and P-V Characteristic Curve

The shading problem will cause the output characteristic curve of the PV system to show multiple peaks, leading to the failure of the traditional maximum power point tracking method. Therefore, it is important to find the global maximum power point quickly and accurately on the multi-peak photovoltaic characteristic curve. The global maximum power point tracking method can effectively distinguish between the local maximum power point and the global maximum power point so that the photovoltaic system can operate at the global maximum power point under multi-peak conditions accurately.

2.4 Overview and Classification of Existing GMPPT Algorithms

In this section, through literature research and analysis, the existing GMPPT algorithms are divided into four categories: the global scanning method, the compound MPPT algorithm based on the conventional algorithm, the mathematical method, and the artificial intelligence method [8]. There are several representative algorithms, with the most types of artificial intelligence algorithms, and the listed in the figure are four more commonly used artificial intelligence algorithms.

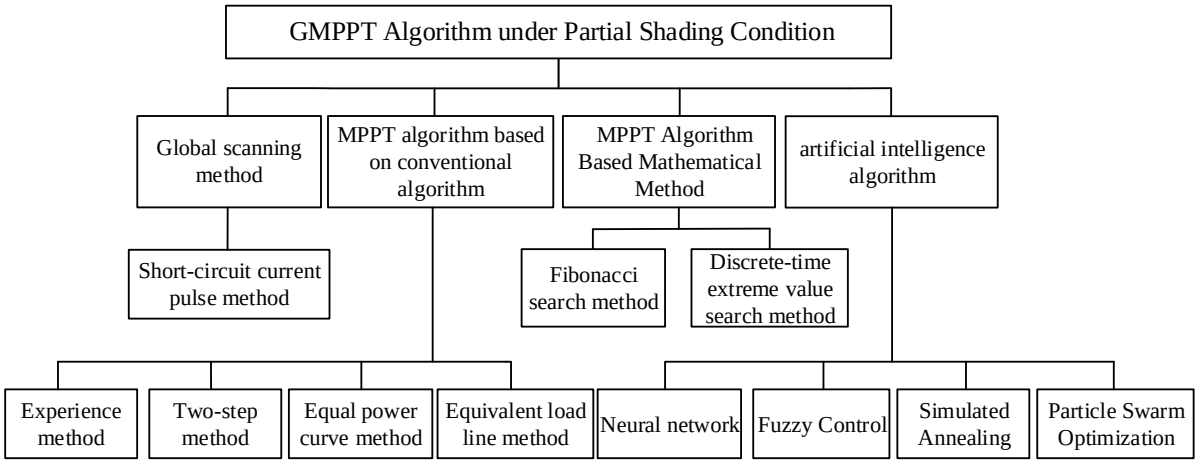

Figure 2-9 GMPPT algorithm classification

2.4.1 Global Scan Method - Short-circuit Current Pulse Method

The global scanning method refers to scanning a power-voltage or power-current curve of a photovoltaic array at a certain frequency to find the voltage, current, or duty ratio corresponding to the global maximum power point, and outputting the voltage value, current value, or the like at the end of the scan. Duty cycle value, and use this value as the corresponding PI control loop command value. For example, the short-circuit current pulse method is to apply a short duration ramp signal to the MOSFET driver connected in parallel with the photovoltaic module in a certain period, so that the equivalent conductance of the MOSFET changes from 0% to 100%. During this period, the power of the photovoltaic array − The current curve is scanned. The global maximum power output of the PV array can be achieved by sampling the global maximum power point current obtained by the scanning and tracking the current value using the PI control loop. The global scanning method needs to scan the power-voltage or power-current curve periodically, the scanning frequency is high, the power loss is greater, but the adaptability to the environmental mutation is stronger.

2.4.2 Traditional Methods—Perturbation Observation Method, Conductivity Increment Method

The MPPT algorithm based on the conventional algorithm refers to first determining the possible range of the global maximum power point of the PV array through some methods, and then using these conventional algorithms such as perturbation observation method or conductance increment method, experience method, two-step method, etc.to accurately track the GMPP.

Empirical method: n*m PV arrays (n is the number of PV modules in series), and the number

of possible LMPPs is n. According to the experience of analyzing the output characteristics of photovoltaic arrays, the voltage corresponding to each LMPP is approximately k*0.85*V_{OC}_module (k=1, 2, 3...N; V_{OC}_module is the open circuit voltage VOC/tandem module of the entire photovoltaic array. The number n can be approximated as the open circuit voltage of each photovoltaic module at 1000 W/m^2, 25V). Therefore, the corresponding LMPP existence interval can be set as: k*[0.75*Voc/n, 0.9*Voc/n] (k=1,2,3,...,n), and then the conventional P&O algorithm is used to track LMPP accurately in these intervals. Finally, the LMPPs tracked in each interval are compared, in which the largest power is GMPP.

This thesis simulates empirical methods. The photovoltaic array consists of three photovoltaic modules connected in series. The parameters (1000W/m^2, 25V) of each photovoltaic module are P_{max}=102W, V_{OC}=14.9V, I_{SC}=8.89A, V_{mpp}=12.4V, and I_{mpp}=8.23A. The illumination of the three photovoltaic submodules is respectively S_1=1000 W/m^2, S_2=800 W/m^2 and S_3=400 W/m^2.

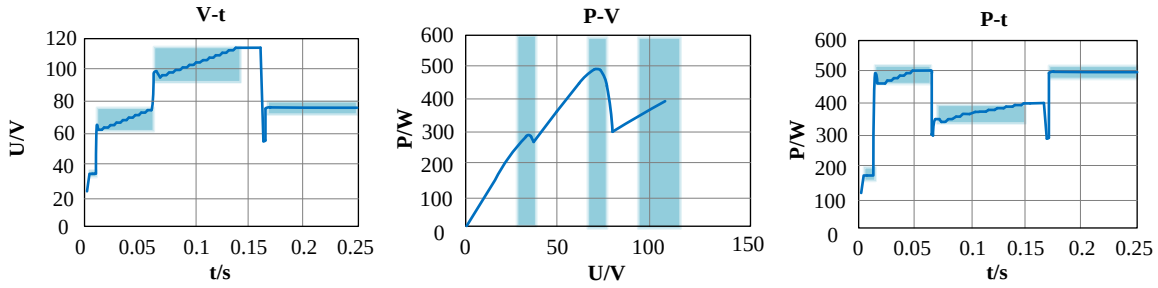

Figure 2-10 Experience simulation results: P-V curve and waveform

The voltage power waveform and P-V curve of the PV array are shown in Figure 2-10. According to the above experience, the three intervals in which LMPP exists are locked. In these three intervals, the P&O algorithm is used to track LMPP, which is 291 W, 504 W, and 395.5 W, respectively. The largest 504 W is GMPP. Finally, using the PI control, the photovoltaic array operated at a voltage corresponding to GMPP of 74V. It can be seen that the empirical method can trace the global maximum power point quickly and accurately. The maximum output power is 504W. However, the disadvantage is that it is necessary to know the number of photovoltaic panels connected in series in the photovoltaic array in advance.

Improved experience method [16]: First, it performs perturbation observation method. After finding a LMPP, according to the voltage parameter of the photovoltaic module at this time, it determines the possible voltage value of another LMPP and adjust the voltage reference

value accordingly. The rules are as follows:

Take three PV modules in series as an example:

1) If the voltages of V_{pv1}, V_{pv2}, V_{pv3} are similar for the three photovoltaic modules, the irradiances of the three photovoltaic modules are considered to be similar, so there is no multi-peak, there is only one peak, which is already found LMPP.

2) If the voltage of a photovoltaic module is less than zero, it is passed by the bypass diode. At this time, adjust the voltage to $0.8*V_{oc}$ and continue the disturbance observation method.

3) If one of the voltages is the lowest and the two are higher, adjust the voltage to $0.8*2/3*V_{oc}$ and continue the perturbation observation method.

4) If there are two lower voltages and one highest voltage, adjust the voltage to $0.8*1/3*V_{oc}$ to continue the perturbation observation method.

In this way, the other LMPP can be found more quickly, and the found LMPP value can be compared to determine the global maximum power point.

The improved empirical method has also been verified by simulation. The photovoltaic array consists of three photovoltaic modules connected in series, one with an irradiance of 1000 W/m^2 and the other two with an irradiance of 400 W/m^2. From the power-voltage (P-V) characteristic curve and the power-time (P-t) characteristic curve of the photovoltaic system, it can be seen that the improved empirical method can track the global maximum power point, i.e. the output power is 2050 W, which effectively utilizes solar energy.

Two-step method: First, it scans large area of photovoltaic array voltage with large step size ΔV to observe disturbances, compares and records the points with the largest power; then use small step Δv near the point to perform perturbation observation method to obtain global maximum power point. We simulated the two-step method using the same PV array parameters and illumination parameters as the empirical method described above. The voltage power waveform and P-V curve are shown in Figure 2-11. It can be seen that the MPPT controller first uses a large step length of 8V as a disturbance observation method, compares the corresponding power values, finds the point where the power is the largest. It continues to do the disturbance observation method with a small step of 0.5V near the GMPP is 504W. It can be seen that two-step method can also track the global maximum power point accurately. The large voltage scan across the entire area can save the tracking time and

improve the tracking speed. The GMPPT can be tracked in only 0.1s.

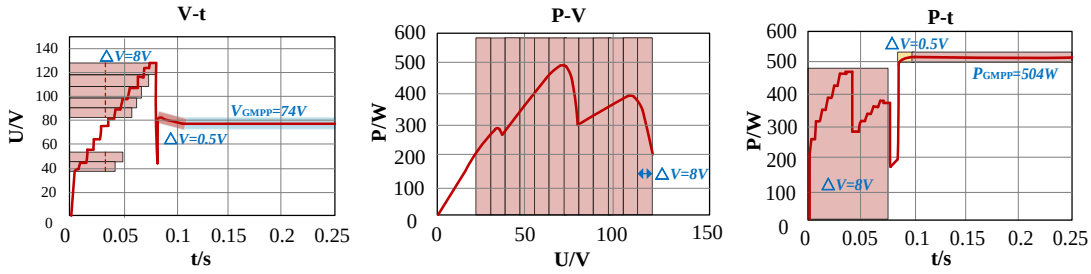

Figure 2-11 Two-step simulation results: P-V curve and voltage power waveform

2.4.3 Mathematical Method

The MPPT algorithm based on the mathematics method refers to that the GMPPT is completed by applying certain mathematical methods to adjust the maximum power point tracking range. Typical algorithms include Fibonacci search and discrete-time extreme search method.

Fibonacci search method [17]: By repeatedly limiting and adjusting the search range, it is ensured that the maximum power point is within the search range. Use the Fibonacci sequence c(n) when adjusting the search range. Take four points V_1, V_2, V_3, V_4 on the PV curve, where $V_3<V_1<V_2<V_4$. The method of narrowing the search range: if $P(V_1)<P(V_2)$, the search range shifts to the right and let $V_3=V_1$, $V_1=V_2$, $V_2=V_2+c(n-1)$, $V_4=V_4$; if $P(V_1))> P(V_2)$, the search range shifts to the left, let $V_3 = V_3$, $V_1 =V_1-c(n-1)$, $V_2 = V_1$, $V_4 = V_2$. When the number of transfers to the same direction continuously reaches twice, the search range is expanded: $V_3=V_1-c(n+2)$, $V_1=V_1$, $V_2=V_2$, and $V_4=V_2+c(n+2)$. It tracks the global maximum power point.

2.4.4 Artificial Intelligence Method

With the development of artificial intelligence technology, artificial intelligence algorithms are applied to the MPPT problem of photovoltaic systems increasingly, mainly including genetic algorithms, BP neural network algorithms, simulated annealing methods, fuzzy control methods, and particle swarm optimization algorithms, etc. [28].

Particle Swarm Optimization algorithm [15]: This algorithm performs iterations to find GMPP through competition and cooperation among population particles. During the search, each particle contains three parameters: current position, velocity, and direction. In each iteration cycle, the particles update their three parameters through two extreme points: the first is the maximum power point that the particle finds at the current moment, and the second

is the entire group finds the maximum power point at the current moment. The particles will adjust the speed and direction according to the historical experience of the entire population of particles, so as to approach the global maximum power point continuously.

Simulated Annealing algorithm [17]: It is necessary to set the initial parameters such as the starting temperature, the ending temperature, and the temperature decreasing rate. At each temperature, the algorithm disturbs the voltage N_T times and measures the corresponding power output P_k. If P_k is greater than the current reference point power P_i, it is accepted as a new reference point; if P_k is less than the current reference point power P_i, then acceptance is determined according to the Metropolis criterion.

$$P_r = exp\left[\frac{P_k - P_i}{T_k}\right] \quad (2\text{-}7)$$

If P_r is greater than 0.1, a new solution less than the current operating output power point is accepted. It is due to the introduction of the mechanism of degradation under power, the simulated annealing method can jump out of the local maximum power point and find the global maximum power point accurately.

2.5 Existing GMPPT Algorithm Comparison and Performance Description

In order to compare the pros and cons of various MPPT algorithms, we can select the appropriate MPPT method. We have selected key performance properties and made clear explanations for them. Further, for the above four categories of MPPT algorithms, we have selected representative algorithms in each category, analyzed and compared them one by one in accordance with the key performance properties that affect the operation of photovoltaic systems. These performance properties can be used as an important reference to evaluate the MPPT algorithm.

In Table 2-3, this thesis gives key performance properties and a brief description. The four properties of the evaluation algorithm, tracking speed, tracking efficiency, tracking GMPP capability, and reliability, are also necessary indexes to consider the performance of the algorithm. A good algorithm should perform well on these four properties. At the same time, we have the following additional explanations for the four performance, i.e. simplicity, efficiency, system dependencies, and costs in the table.

2.5.1 Simplicity

The simplicity of the algorithm depends on the number of physical quantities measured by the sensors in the photovoltaic system and the number of parameters in the MPPT function. For the empirical method, its simplicity can be almost equal to the perturbation observation method (only a few search scopes in the function), so the application of the empirical method is very simple. Similarly, for the two-step method, the steps it adds to the perturbation observation method are only the initial large step global scan [27], followed by the perturbation observation method, so it is also very simple. On the contrary, for the Fibonacci sequence search method, because it needs to use the Fibonacci sequence and needs to store the power and voltage information of the four operating points, its implementation becomes more complicated.

Table 2-3 MPPT main performance properties and specific instructions

Algorithm performance	Specific instructions
Tracking speed	GMPPT algorithm tracking convergence speed.
Tracking efficiency	The ratio of the output efficiency of the photovoltaic system to the ideal maximum power.
Steady-state oscillation	Voltage and power oscillations at steady state.
System dependencies	Does it depend on the parameters of the system other than the open circuit voltage, such as the number of photovoltaic panels in series.
Simplicity	It depends on the number of parameters required by the algorithm, the number of variables, and the code length.
Reliability	The probability of tracking the global maximum power, that is, the ratio of the number of times tracked to the total number of trials.
Cost	The number of sensors and the number of microprocessors. If the analog method does not require a microprocessor, the cost is lower.
Track GMPP capabilities	Whether to trace the global maximum power point
Tracking accuracy	the accuracy of the global maximum power point tracking method

2.5.2 Work efficiency

Efficiency is defined as the ratio of the output power of the photovoltaic system to the maximum power possible. Because the short circuit current pulse method requires a periodic global scan of the power-voltage curve, the higher the scan frequency, the greater its power loss [20]. In order to respond to changes in the external environment, this algorithm needs to increase the scanning frequency. Therefore, its efficiency is not very high. For the

empirical method, if the disturbance step length in the steady state is very small, the power loss caused by the steady state disturbance is negligible and has high efficiency. For simulated annealing, because it does not have steady-state oscillations and does not require a periodic scan of the power-voltage curve, it has a very high efficiency. Work efficiency is usually the most important reference condition for evaluating an algorithm.

2.5.3 Hardware costs

Although it is difficult to calculate the cost of the system accurately before building the entire hardware platform, we can roughly estimate the cost of implementing the algorithm [21], mainly based on the number of sensors used by the algorithm and the number of microprocessors. For empirical methods and simulated annealing, their algorithms only require a voltage sensor, a current sensor, and a microprocessor unit in the implementation. For the short-circuit current pulse method, due to the additional DC-DC converter and microprocessor unit, its hardware cost is much higher than other global maximum power point tracking methods [22].

2.5.4 System Dependence

If GMPPT algorithm needs to know other information besides the open circuit voltage of the PV system, then we call this algorithm system dependent. For the empirical method, it needs to know the number of PV modules in series to calculate the tracking area, so it is system dependent. Some algorithms require information on the type of DC-DC converters. The MPPT algorithm for SEPIC converters proposed in [23] is applicable only to specific single DC-DC converter types. It has strong system dependencies, but not a wide range of application capabilities.

From the previous discussion, we analyzed and compared the advantages and disadvantages of each algorithm under the evaluation of performance properties, and gave a degree of conclusions about the merits of each algorithm. Then we summarized the conclusions in the table 2-4.

Table 2-4 Comparison of Global Maximum power point tracking methods

Algorithm performance	Experience method	Two-step method	Short-circuit current pulse method	Fibonacci search method	Particle Swarm Optimization	Simulated Annealing
Tracking speed	fast	quickly	fast	general	general	quickly
Tracking efficiency	high	high	medium	high	Very high	high
Steady-state oscillation	Have	Have	no	no	no	no
System dependencies	Have	no	no	no	no	no
Simplicity	simple	simple	Moderate	complex	Moderate	Moderate
reliability	high	high	high	medium	medium	high
cost	low	low	high	low	low	low
Track capabilities	Have	Have	Have	Have	Have	Have
Tracking accuracy	medium	low	medium	medium	high	medium

From the above table, it can be found that traditional algorithms such as empirical method, two-step method, and short-circuit current pulse method have certain disadvantages in different performance properties. The artificial intelligence algorithm performs well in each index, using particle swarm optimization and simulated annealing. The performance of the method is better than other algorithms. The simulated annealing algorithm has a high tracking accuracy, and the PSO algorithm has a fast tracking speed. Therefore, we consider combining the two algorithms. If we can get a mixed algorithm [38], we can make the overall tracking performance better.

2.6 Summary of This Chapter

This chapter gives an overview of the principle of photovoltaic arrays, analyzes the phenomenon of causing localized multi-peak shielding and gives solutions. This chapter tests the output characteristics of photovoltaic arrays under multi-peak conditions. Then this chapter systematically classifies the existing GMPPT algorithms and introduces the representative GMPPT algorithm in each category in detail, simulates some of the common algorithms to obtain waveforms. Finally, a comprehensive list of key parameters affecting the performance of the PV system's maximum power point tracking method is provided and explained in details. According to these key properties, comprehensive comparisons are made between several typical GMPPT algorithms, which is an important reference for selecting suitable algorithms.

Through the preliminary comparison in this chapter, we can find that the simulated annealing algorithm and the Particle Swarm Optimization algorithm have their own advantages. These two algorithms perform better than the traditional algorithms and other artificial intelligence algorithms. If we can combine the advantages of the two algorithms, the overall improvement of GMPPT efficiency must be an improvement. This thesis will introduce these two algorithms in detail in the next chapter.

3 RESEARCH ON PROPOSED SA+PSO ALGORITHM GMPPT METHOD

According to the comparison and analysis of existing global maximum power point tracking method in chapter 2, although MPPT algorithm can detect the output maximum peak value of PV array, the output global maximum power is still smaller than the ideal maximum power of PV array. It means the sum of output maximum power of each photovoltaic module. Now traditional MPPT algorithm fails to solve the multi-peak problem.

In order to solve the multi-peak problem, this thesis begins with GMPPT algorithm focusing on the artificial intelligence method. Among them PSO algorithm searches fast, but the convergence accuracy is low. SA algorithm has the ability to jump out of local maximum point because it accepts poor points with a certain probability, but the search time is long. This thesis combines these two algorithms. First it uses PSO algorithm to execute global search in the search space, then SA algorithm executes local search to find the final solution. In this thesis, the proposed SA+PSO mixed algorithm is verified by software simulation. The advantages of the algorithm are analyzed in three aspects: tracking accuracy, tracking time, and self-restart capability.

3.1 Existing PSO and SA Algorithm Analysis

Particle swarm optimization algorithm is originally simplified from the social model. Many animals have a certain group behavior in nature. Usually group behavior can be modelled by simple rules (fish, birds, etc.). Although each individual has very simple rules of behavior, group behavior can be very complicated. In 1986, Frank Heppner proposed the bold (bird-oid) model [26] in order to simulate the characteristics of the population accurately in the natural world. Later in the research, habitat restrictions added to the model. It means the range of organisms in the model could not exceed the set habitat range. Inspired by this model, people proposed a new type of intelligent optimization algorithm, which called

Particle Swarm Optimization algorithm. The idea directly derived from the bird's foraging behavior in nature. [24]. In the research of bird foraging behavior, researchers found that during the process of foraging, birds will suddenly gather, suddenly spread out and suddenly change their foraging direction. It is impossible to predict the behavior of birds accurately. But in further research, birds have been found to have overall consistency. Individuals and individuals in birds have always maintained a suitable distance. Through the study of some similar biological groups in nature, it is found that there is a mechanism for sharing social information with each other within the group. It provides an advantage for the evolution of the group, which is the basis of the PSO algorithm.

PSO algorithm is suitable for global maximum power point tracking under multi-peak conditions. It can guide populations to optimize search intelligently through the competition between particles and populations generated by population particle cooperatively. The optimization problem is to search the solution space of the particles. Each particle runs at a certain speed in the search space. The speed of the particles needs to be adjusted dynamically according to its own flight experience and the flight experience of other particles. In each iteration, each particle determines the appropriate objective function value. The particle updates its position and velocity with two maximum values. The first is the optimal solution until the particle itself finds the current moment, known as P_{best}; the other is the optimal solution found at the current moment in the entire population, known as G_{best}. The speed update formula with P_{best} and G_{best} calculates as follows.

$$v_{\text{i}}^{k+1} = wv_{\text{i}}^{k} + c_1 r_1 \left(P_{\text{best}} - S_{\text{i}}^{k}\right) + c_2 r_2 \left(G_{\text{best}} - S_{\text{i}}^{k}\right) \tag{3-1}$$

$$S_{\text{i}}^{k+1} = S_{\text{i}}^{k} + v_{\text{i}}^{k+1} \tag{3-2}$$

Due to its good performance under multi-peak conditions, the particle swarm optimization algorithm is widely used in photovoltaic arrays. Particle swarm optimization has the advantages of parallel processing and good robustness. Moreover, the probability of tracking the global maximum power point is high, and the computational efficiency is higher than that of the traditional stochastic method. The biggest advantage of this method lies in its simple implementation.

The initial position of the PSO algorithm can generate randomly or set manually. Then it iterated according to formula (3-1) and formula (3-2). In order to improve the search efficiency, the particles can place at the point where the local optimum solution occurs based

on the analysis of the P-U output characteristic curve of the PV array. Reference [32] shows that for M×N photovoltaic arrays, there are at most N local maximum power points. If the open voltage of the array under uniform illumination is U_{oc}, then the initial position of the i particle can be obtained as follows:

$$S_i^0 = \frac{i \cdot U_{oc}}{N+1} \tag{3-3}$$

The search range for particles is 0 to U_{oc}.

The stop conditions of the general particle swarm optimization algorithm are achieved by presetting the number of iterations. However, for the PV array MPPT algorithm, few iterations will affect the accuracy of the optimal value. In the contrary excessive iteration will result in low efficiency. Repeatedly iterating will bring long-time power fluctuations. In order to stabilize the power to the maximum power point as quickly as possible, this thesis adopts the following termination strategy:

Since the position of the particles disperse in the initial stage of the algorithm, when a location is very concentrated, it can be considered that the maximum power point has been reached. This thesis proposes that when the maximum position difference between particles is less than $0.005U_{oc}$ [34] and the iteration stopped, it can be considered that the global optimal solution is the largest one of the best fitness values for all particles at that moment.

The standard PSO algorithm process:

*step*1: Initializes a group of particles, including random position and velocity;

*step*2: evaluate the fitness of each particle;

*step*3: For each particle, compare its fitness value with its best position P_{best}. If it is better, it will be the current best position G_{best};

*step*4: For each particle, compare its fitness value with its best position G_{best}. If it is better, it will be the current best position G_{best};

*step*5: Adjust the particle velocity and position according to (3-1) and (3-2);

*step*6: Turn to step2 if the end condition doesn't reach.

The iterative termination condition generally selects the maximum number of iterations according to the specific problem and the optimal position searched for by the particle swarm group so far satisfies the predetermined minimum adaptive threshold.

The flow chart of the PSO algorithm is as follows:

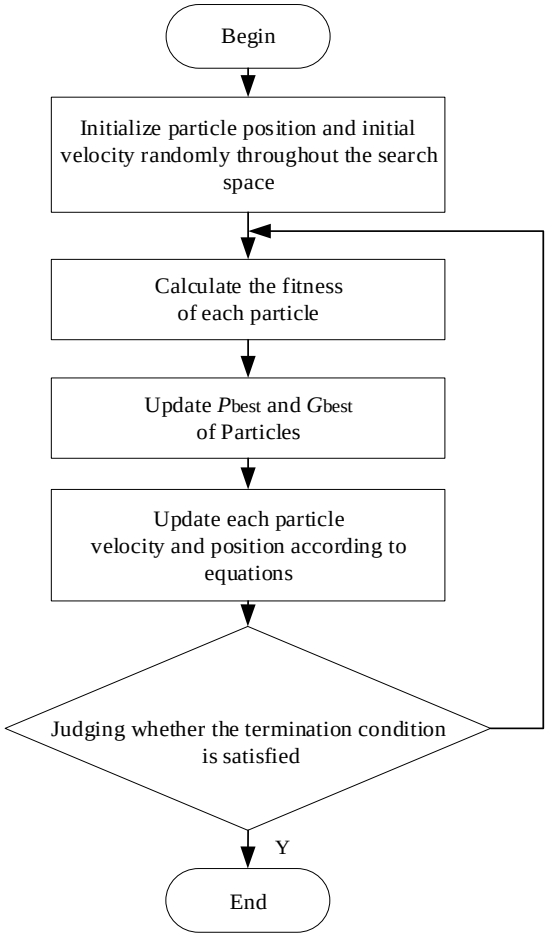

Figure 3-1 Global Maximum power point tracking Based on Particle Swarm Optimization

The following describes the existing simulated annealing algorithm. Simulated annealing is inspired by the cooling crystallization behavior. In general, the crystal will reach the lowest energy state during this process [25]. It is necessary to set initial parameters such as starting temperature, ending temperature and temperature decreasing rate, and so on.

At each temperature, the algorithm disturbs the voltage N_T times and measures the corresponding power output P_k.

*step*1: Set the initial parameters: initial temperature T, temperature drop rate α and end temperature T_{min}.

*step*2: Select a random voltage V_i in the working range and measure the corresponding power P_i.

*step*3: When the temperature T is higher than the end temperature T_{min}, repeat the following steps:

a) Selecting a random voltage V_k, and measuring the corresponding power P_k.

b) If $P_k > P_i$, Vk is accepted as a new operating point, i.e., $V_i = V_k$.

c) In the opposite, if $P_k < P_i$, then whether to accept V_k as a new operating point is determined by the acceptance probability in equation (3-1).

d) If four voltage disturbances have been performed at the current temperature, decrease the temperature according to equation (3-2).

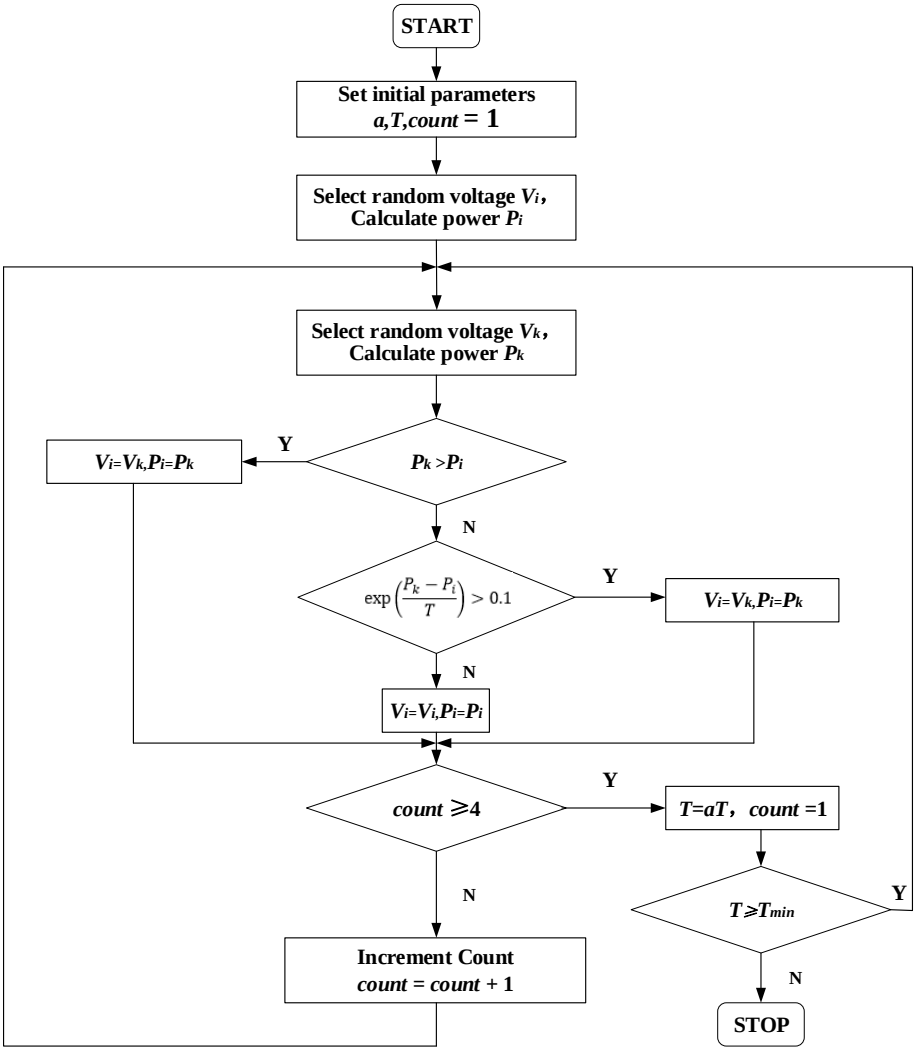

Figure 3-2 Global Maximum power point tracking Based on Simulated Annealing

The flow chart of the simulated annealing method is figure 3-2.

Simulated annealing has a global search capability and cannot be limited to local maximum power points.

3.2 Flowchart of GMPPT Based on SA+PSO Algorithm

Particle swarm algorithm can track the maximum point of the static multi-peak curve. The convergence speed is fast, but the convergence accuracy is low. The SA algorithm accepts poor points with a certain probability, so it has the ability to jump out of local optima, but the search time is long. In addition, the step of voltage update leads to a lot of power loss and longer tracking time. Therefore, this thesis proposes a global maximum power point tracking method based on SA+PSO mixed algorithm. The proposed SA+PSO mixed algorithm combines the advantages of the two methods. It does not depend on the initial value, changes the way of the step length updating. It jumps out of the local maximum power point, and tracks the global maximum power point more accurately. Therefore, it is easy to solve the aforementioned problem. The global maximum power point tracking method of the SA+PSO mixed algorithm is also applicable to different photovoltaic systems.

This thesis embeds the principle of PSO algorithm into SA algorithm. Firstly, PSO algorithm does global search in the search space. Then the individual optimal solution obtained by PSO is used as the initial solution of SA. Finally SA performs local search to find the final solution. The values of inertia weight and individual learning factors are the main part of the SA+PSO algorithm.

The global maximum power point tracking method based on the SA+PSO mixed algorithm needs to be set in advance, including the start temperature, end temperature, and temperature decrease rate. At each temperature, the algorithm perturbs the voltage multiple times and calculates the corresponding output power. Then it compares the new operating point power with the current reference power. If the new operating point has more power, it will be accepted as a new reference point. If the new operating point has less power, it does not change. It depends on the acceptance probability, Metropolis criterion, which related to the energy difference and the current search temperature. The acceptance probability is given in (3-3). P_{k} is the power at the current voltage, P_i is the power of the previous operating point, and T_{k} is the current temperature of the system. Obviously, power reduction under higher temperatures is likely to be accepted. As the temperature decreases, the possibility of accepting lower power also decreases.

$$P_{\mathrm{r}} = exp[\frac{P_{\mathrm{k}} - P_{\mathrm{i}}}{T_{\mathrm{k}}}] \tag{3-4}$$

The geometric cooling method is as follows:

$$T_{\mathrm{k}} = \alpha T_{\mathrm{k-1}} \tag{3-5}$$

T_k is the temperature in step k, which is the rate of temperature decrease ($0<\alpha<1$). The flowchart and algorithm process ares as follows:

step 1: Set initial value: including start temperature T_0, temperature decrease rate α and end temperature $T_{\min}$, *step*, *flag*, N_S and N_T;

step 2: Select the operating point voltage V_1 randomly between the zero point and the open circuit voltage V_{OC};

step 3: Calculate the power P_i related to the operating point on the P-V curve;

step 4: $step=w\times step+c_1 * r_1 (U_{\max}-U_{\mathrm{ref\_out}})$, where w is the inertia factor and c_1 is the individual learning factor;

step 5: $V_k = V_i + step$, and calculate the P_k associated with V_k;

step 6: When the temperature is higher than the end temperature, repeat the following steps:

a) Generate a random voltage V_k;

b) Calculate the power P_k associated with the operating point of the P-V curve, increase the perturb count;

c) When P_k is larger than P_i, the operating point updates, which means $P_i = P_k$, $V_i = V_k$; if P_k is larger than $P_{\max}$, then $P_{\max} = P_k$ updates, $V_{\max} = V_k$; then increase the accept number.

d) In the opposite, when P_k is lower than P_i, the operating point updates due to the acceptance rate of formula (3-4). If accepted, the accept count increases.

e) Cooling temperature after N_T step changes. Restart and set $V_i = V_{\max}$.

step 7: When the stop condition is satisfied, the algorithm stops the voltage disturbance and waits for restart.

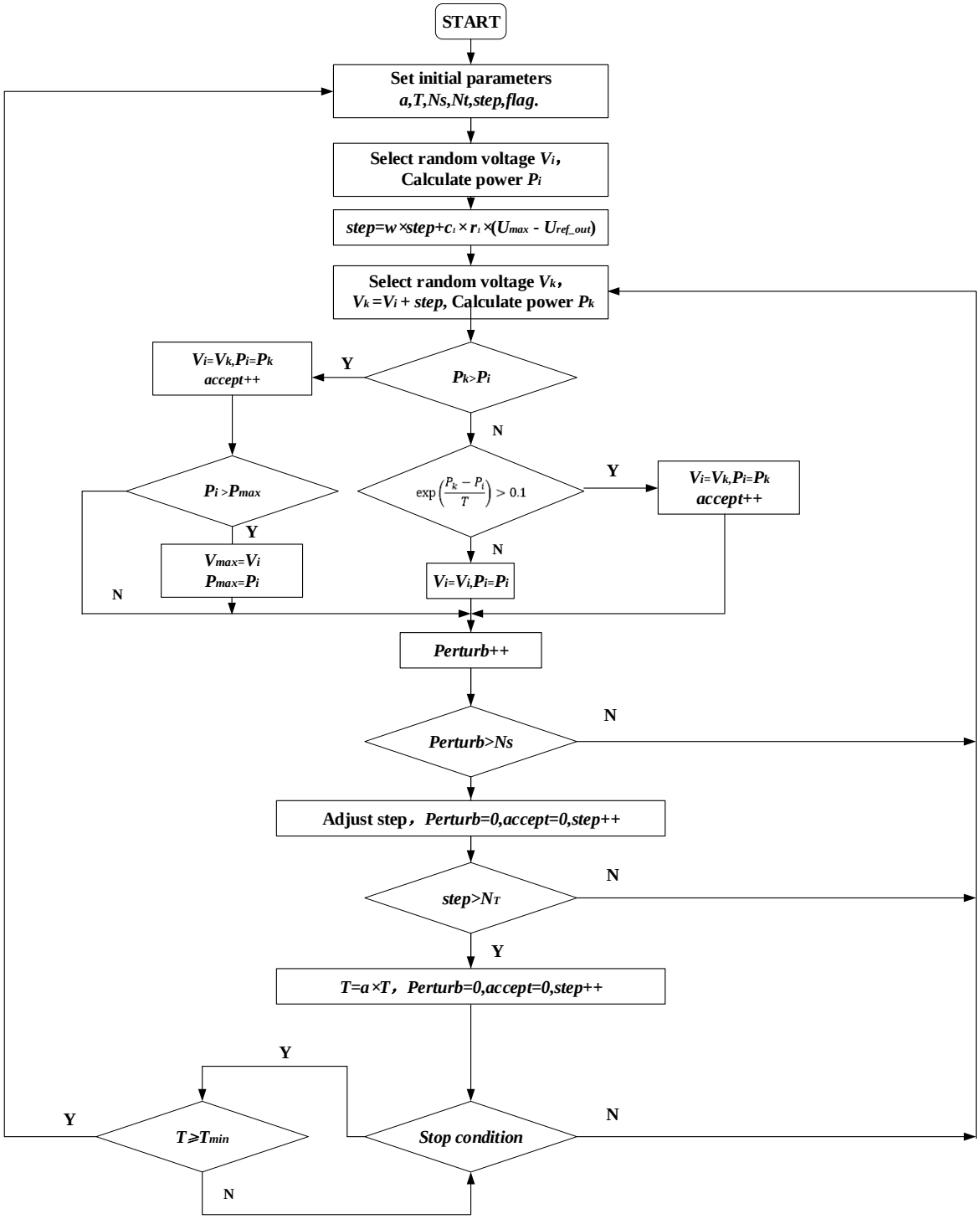

Figure 3-3 Flowchart of the SA+PSO mixed algorithm

3.3 Simulation and Verification of GMPPT Method Based on SA+PSO Mixed Algorithm

In order to verify the performance of the proposed method, the thesis simulates in MATLAB/Simulink, and uses a photovoltaic panel to connect a resistive load through a Boost circuit. First, SA+PSO mixed algorithm tracks the maximum power point under single-peak condition. Then SA+PSO mixed algorithm operates under multi- peaks condition. Finally, SA+PSO mixed algorithm operates under multi-peak and irradiance changing condition. .

The first single-peak experiment is a basic experiment. It not only considers whether the algorithm can track the maximum power point, but also consider the time algorithm takes to track the maximum power point. If the tracking time is too long, such an algorithm is difficult to adopt on a large scale in practical industrial applications. The comparison of the tracking time will be further explained in section 3.4 of this chapter.

The experiment used a photovoltaic panel with an irradiance of 800 W/m^2. There is only one peak point. The maximum power is 700 W, the maximum power point voltage is 104V, and the open circuit voltage is 150 V. The P-V characteristic of the photovoltaic panel at this moment is shown in Figure 3-4:

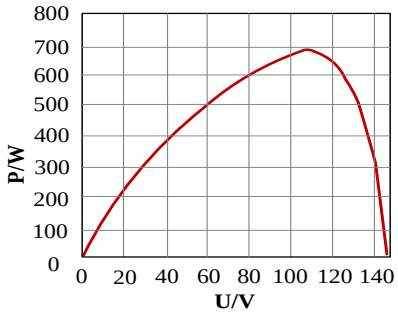

Figure 3-4 P-V characteristics of photovoltaic panels

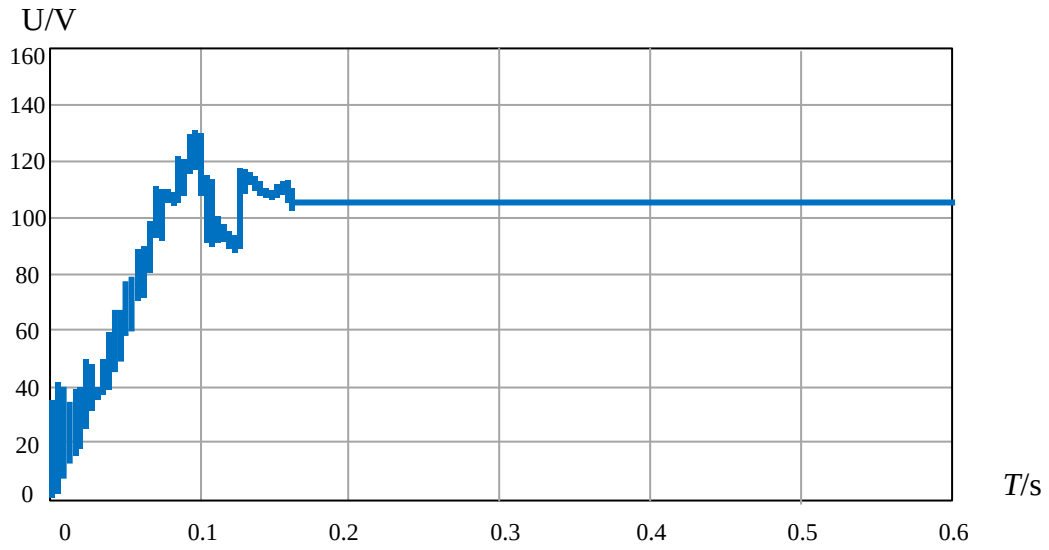

(a) Photovoltaic panel output voltage curve

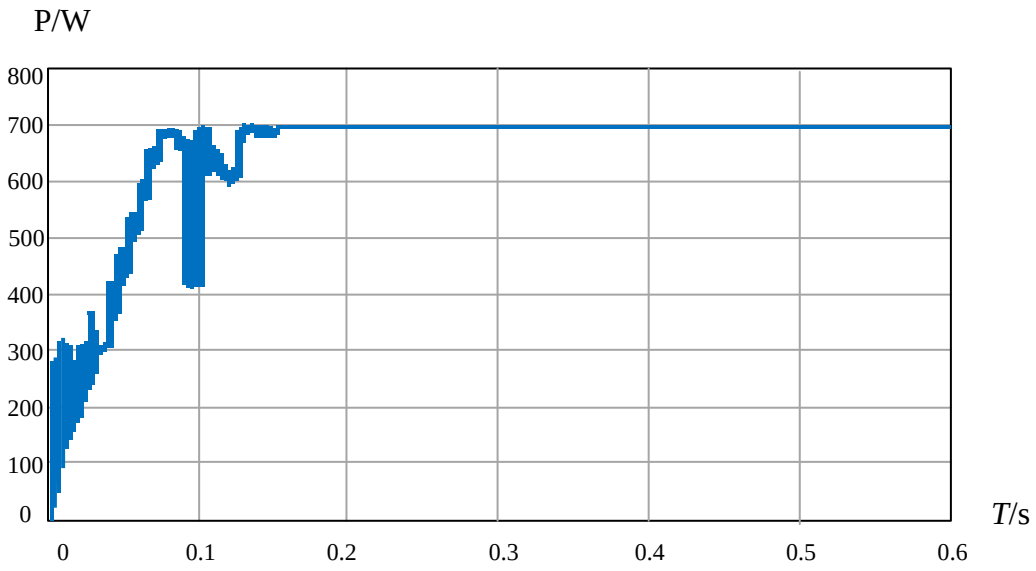

(b) Photovoltaic panel output power curve

Figure 3-5 PV output voltage (up) and output power (down) curves

The final output voltage waveform is shown in Figure 3-5. The output voltage traces to 104V at 0.16s and the output power is traced to 700W. The maximum power point coincides with Figure 3-4, which shows the characteristics of the photovoltaic panel. Therefore, SA+PSO mixed algorithm can track the global maximum power under single-peak condition.

After the algorithm has tracked the maximum power point under single-peak conditions, the second experiment uses three photovoltaic panels. SA+PSO mixed algorithm is used for simulation under multi-peak conditions.

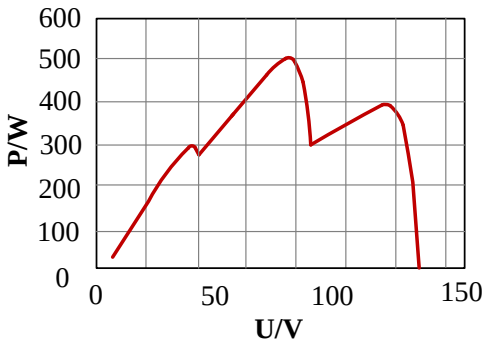

Figure 3-6 Photovoltaic panel characteristics

The irradiance of three photovoltaic panels are: S_1 = 1000 W/m^2, S_2 = 800 W/m^2, and S_3 = 400 W/m^2. The P-V characteristic curve of the photovoltaic panel at this moment is shown in Figure 3-6. There are three peaks. The global maximum power point voltage is 74V, the maximum power is 500W, and the open circuit voltage is 120V. Figure 3-7 shows the output voltage and output power of the photovoltaic panel.

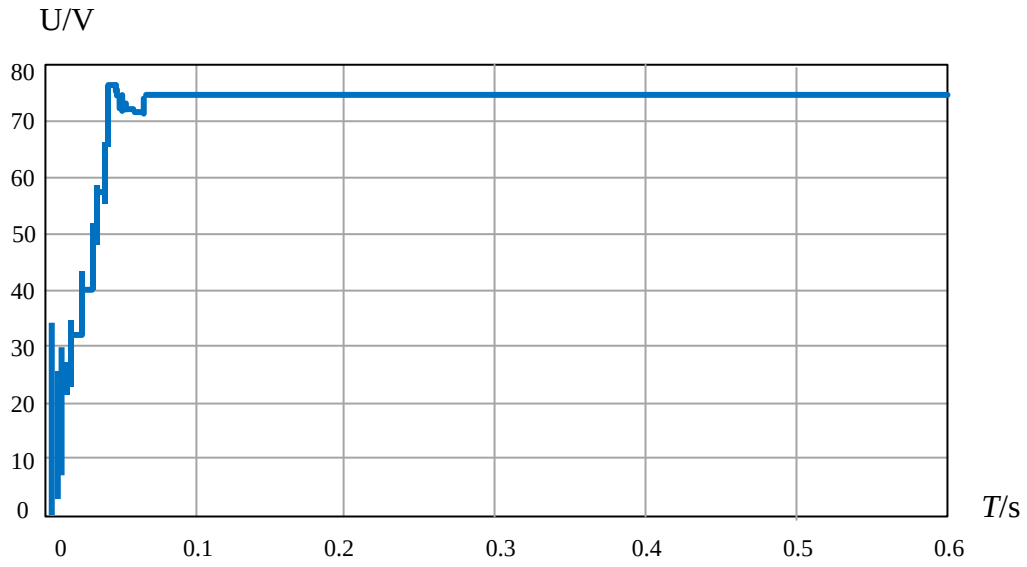

(a) Photovoltaic panel output voltage curve

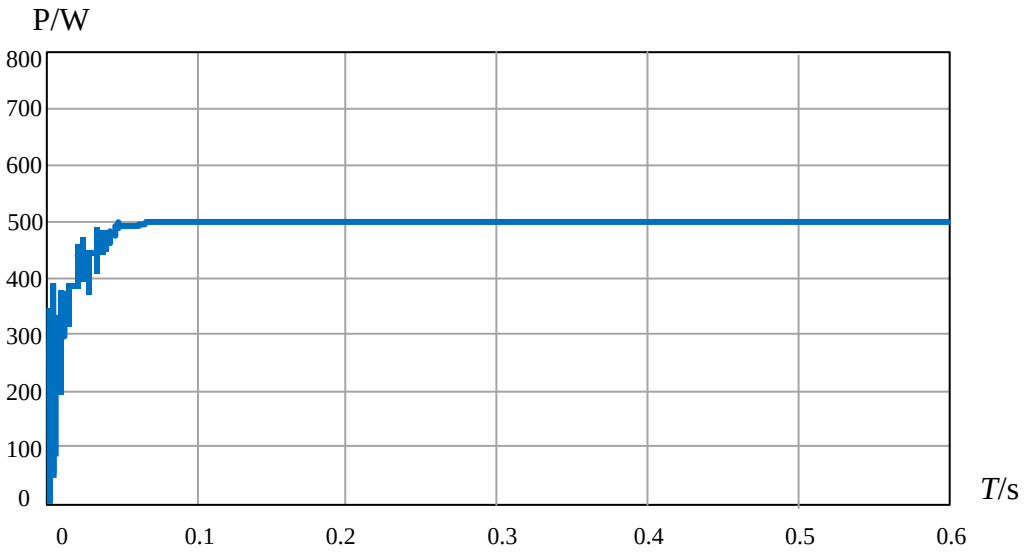

(b) Photovoltaic panel output power curve

Figure 3-7 PV output voltage (up) and output power (down) curves

From Fig. 3-7, it can be seen that the output voltage is stable at 74V at 0.05s, and the output power is stabilized at 500W, which is consistent with the maximum power on the characteristic curve of the photovoltaic panel given in Fig. 3-6. So the algorithm can track the global maximum power point under multi-peak conditions. Next, the SA+PSO mixed algorithm is applied in the case of irradiance changes condition.

In the third experiment, three photovoltaic panels are used. The irradiance of three photovoltaic panels are: S_1 = 1000 W/m^2, S_2 = 800 W/m^2, S_3 = 400 W/m^2. At 0.25 s, irradiance changes occur on the photovoltaic panel 1 : S_1 drops from 1000 W/m^2 to 400 W/m^2. S_2 and S_3 remain unchanged. For w and c_1, we choose w = 1.1, c_1 = 1.65, and c_2 = 1.45.

Figure 3-8 shows the P-V characteristics of photovoltaic panels. Before the change of irradiance, the photovoltaic panel has three peaks with a maximum power of 500 W. After the irradiance changes, the photovoltaic panel has two peaks with a maximum power of 360 W. From the figure, the global maximum power reduces from 500W to 360W, and the maximum power point voltage changes from 74V to 105V after the irradiance changes.

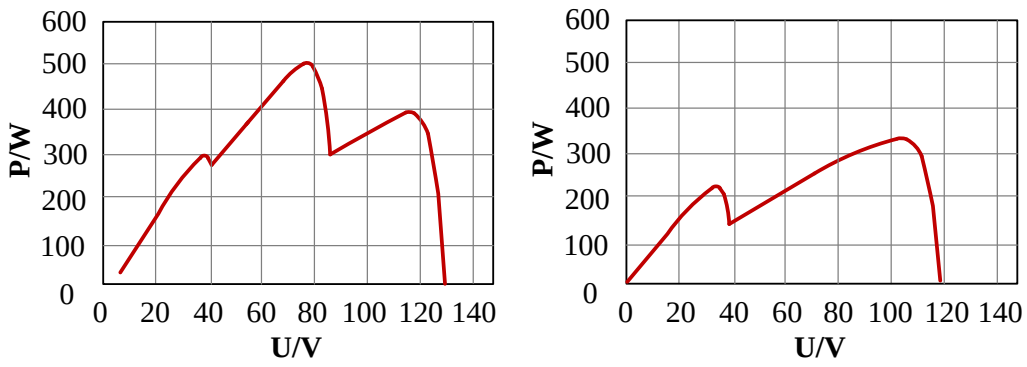

Characteristic curve before 0.25 s; Characteristic curve after 0.25 s

Figure 3-8 Output characteristics before and after the change of the photovoltaic panel

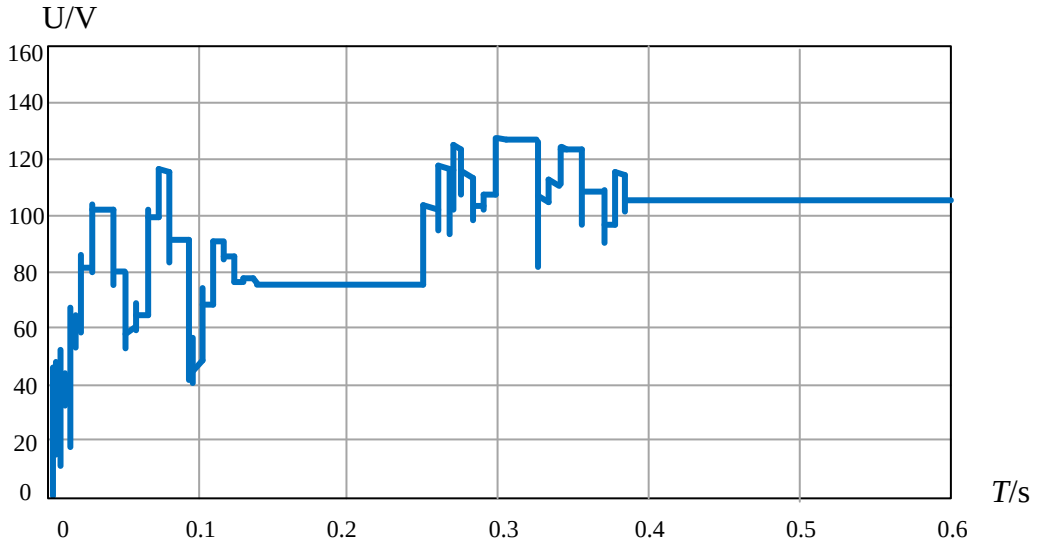

(a) Output voltage curve

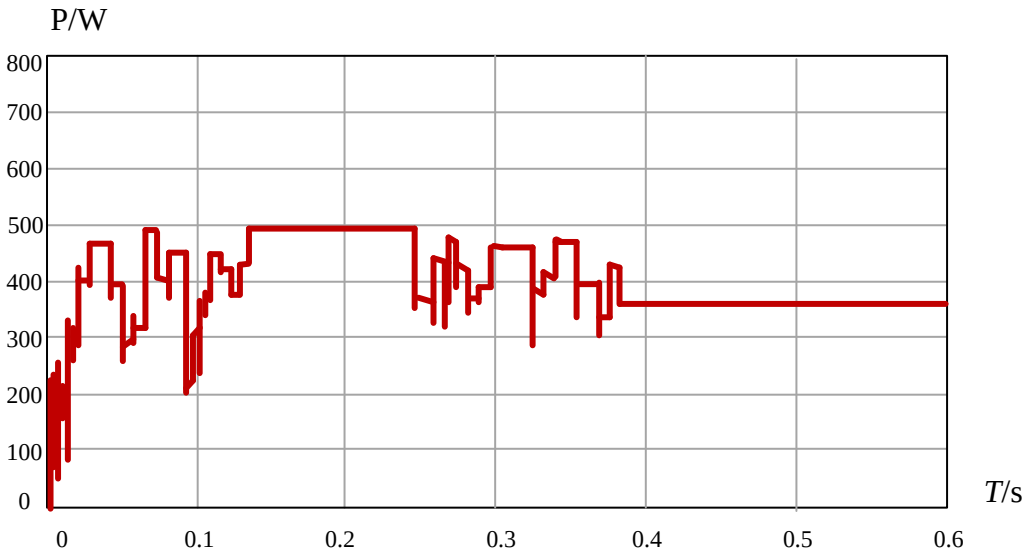

(b) Output power curve

Figure 3-9 Output power and reference time

The voltage output of the photovoltaic system and its reference voltage is shown in Figure 3-9.

From Figure 3-9, SA+PSO mixed algorithm can track the global maximum power of 500W and the global maximum power point voltage 74V at 0.13s. When time reaches 0.25s, the irradiance changes and one of the photovoltaic panels drops from 1000W/m^2 to 400W/m^2. At this point, SA+PSO algorithm can restart automatically and spend 0.12s tracking the global maximum power of 360W again. It stabilizes at the global maximum power point voltage of 105V. This means that comparing to the existing algorithms, the SA+PSO mixed algorithm not only implements a self-restart function, but also has a fast tracking time.

When SA+PSO algorithm compared with existing SA algorithm, SA+PSO algorithm has a faster convergence speed and can search for a new optimal operating point quickly. SA algorithm [24] needs at least 0.3s to track the global maximum power point, but SA+PSO algorithm can reduce the tracking time to 0.12s ~ 0.13s.

3.4 Using SA+PSO Mixed Algorithm to Improve the Performance of Photovoltaic System

This section continues doing simulation for SA+PSO mixed algorithm. Then we conducts in-depth research on the algorithm. SA+PSO mixed algorithm is compared with the existing simulated annealing algorithm and the enhanced simulated annealing method. The comparison is from three aspects: self-restart capability, convergence time and convergence accuracy. It is verified that SA+PSO algorithm can be faster compared with the existing Simulation Annealing and Enhanced Simulated Annealing (ESA) algorithm in the tracking speed. The tracking accuracy of SA+PSO algorithm is higher.

3.4.1 Self-restart Capability

In order to ensure the validity of the comparison, the experiment controlled the external conditions to be same. The output characteristics of the photovoltaic panels before and after irradiance changing are the same. And the time for controlling the irradiance changing is the same [37]. SA+PSO algorithm is compared with the existing simulated annealing algorithm and the enhanced simulated annealing method. Firstly, the performance of the three algorithms is compared from the self-restart capability.

The thesis controlled the irradiance changing time is 0.4s. Figure 3-10 shows the

characteristics before and after the photovoltaic panel irradiance changes. The output voltage curve of the photovoltaic panel is shown in Figure 3-10 below, where (a) SA algorithm, (b) Enhanced SA algorithm, (c) SA+PSO algorithm.

Before the sudden change of irradiance, three algorithms can track the global maximum power point accurately. The tracking time of SA algorithm is 0.32s, the tracking time of ESA algorithm is 0.28s, and the tracking time of SA+PSO algorithm is 0.15s. The speed of SA+PSO algorithm is the fastest. After the sudden change of irradiance, SA algorithm fails that is no self-restart ability; ESA algorithm has self-restart ability after the irradiance changes, but the tracking speed becomes slower, and the tracking time needs 0.22s after perturbation operated again; SA+PSO algorithm can still maintain the original tracking speed after the irradiance changes. The algorithm tracks the global maximum power point accurately again at a disturbance of 0.13s. At the same time, SA+PSO algorithm has a faster tracking speed and spends less tracking time than the other two algorithms. Through this comparison experiment, SA+PSO algorithm has obvious advantages. The tracking speed is faster while ensuring accuracy. SA+PSO algorithm has a high accuracy.

The following figure shows the output voltage vs. time (V-t) curves of the existing SA algorithm, ESA algorithm, and SA+PSO algorithm. From the figure, the proposed SA+PSO algorithm in this thesis can track the global maximum power point faster. The self-restart capability has improved significantly after the irradiance changes. The actual global maximum power point can be tracked again accurately.

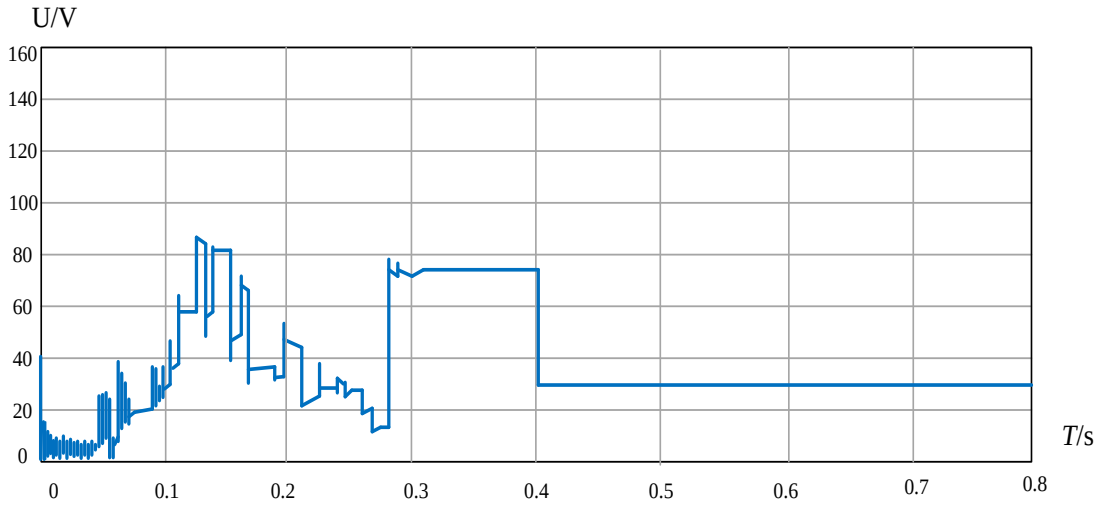

(*a*) SA Algorithm

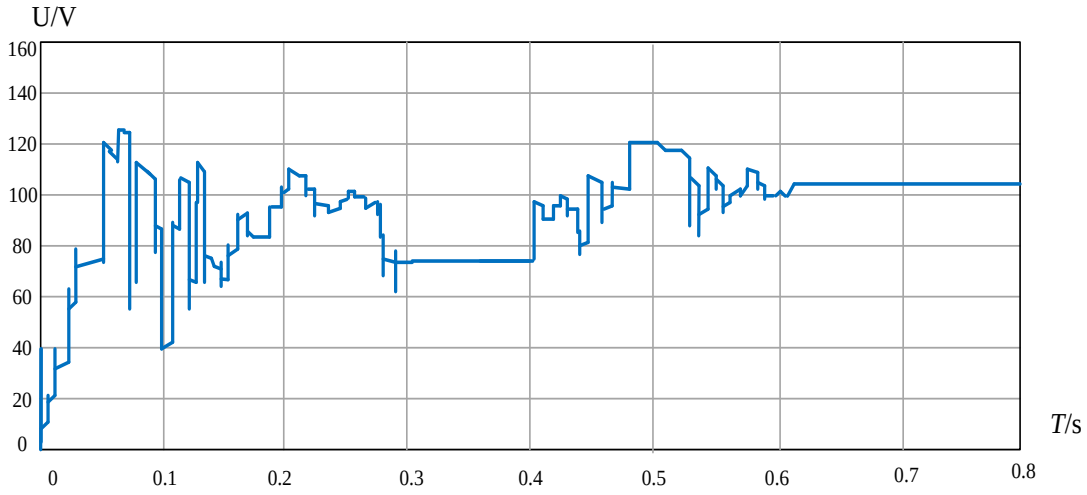

(*b*)Enhanced SA Algorithm

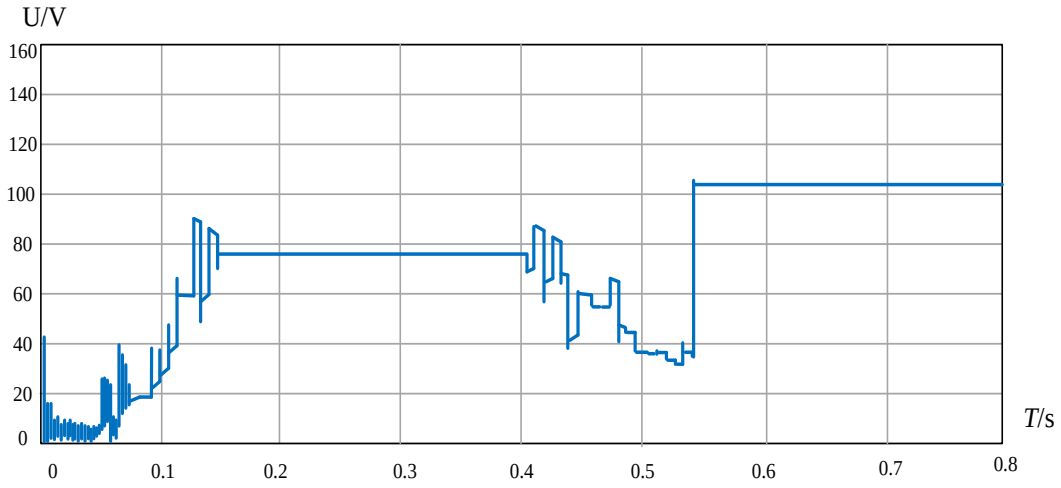

(*c*)SA+PSO mixed Algorithm

Figure 3-10 GMPP tracking waveforms of three algorithms before and after light mutation

3.4.2 Tracking Time

In order to verify the tracking speed of the three algorithms, this thesis carries out 50 simulations and analysis of the three algorithms respectively. Then we summarize the chart below. In order to prove the tracking speed of the SA+PSO mixed algorithm, the experiment does 50 iterations. Finally, we compare the tracking time between SA+PSO mixed algorithm (orange line) and the existing SA algorithm (blue line) statistically.

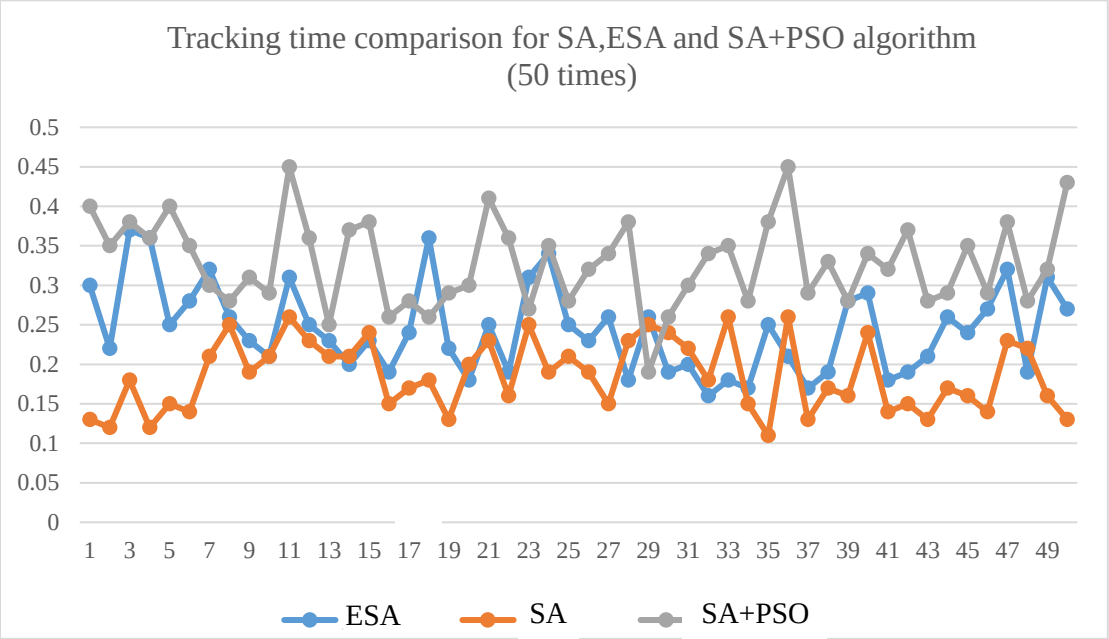

Figure 3-11 Comparison of SA, ESA, SA+PSO mixed algorithm tracking time 50 times

From Figure 3-11 we can see that the proposed SA+PSO algorithm in this thesis can reduce the tracking time greatly. Compared with existing methods, the tracking speed of SA+PSO algorithm has significant advantages.

3.4.3 Tracking Accuracy

In order to verify the tracking accuracy, this chapter analyzes the convergence of the three algorithms and summarizes the pie chart, as shown in Figure 3-12.

By analyzing and summarizing the pie chart, SA+PSO algorithm has a very high convergence accuracy. It is superior to the existing simulated annealing algorithm and enhanced simulated annealing algorithm. This thesis compares these three algorithms together because the efficiency of SA algorithm and ESA algorithm are in the front rank of the artificial intelligence algorithm so far. Therefore, if the proposed algorithm in this thesis is better than these two algorithms, it must be better than other conventional algorithm.

SA+PSO algorithm also improves the convergence accuracy. It can converge the accuracy to 95%, which compare to 93% of the existing SA algorithms. And it improves the 1% convergence accuracy to 10%. This is the best among the three algorithms.

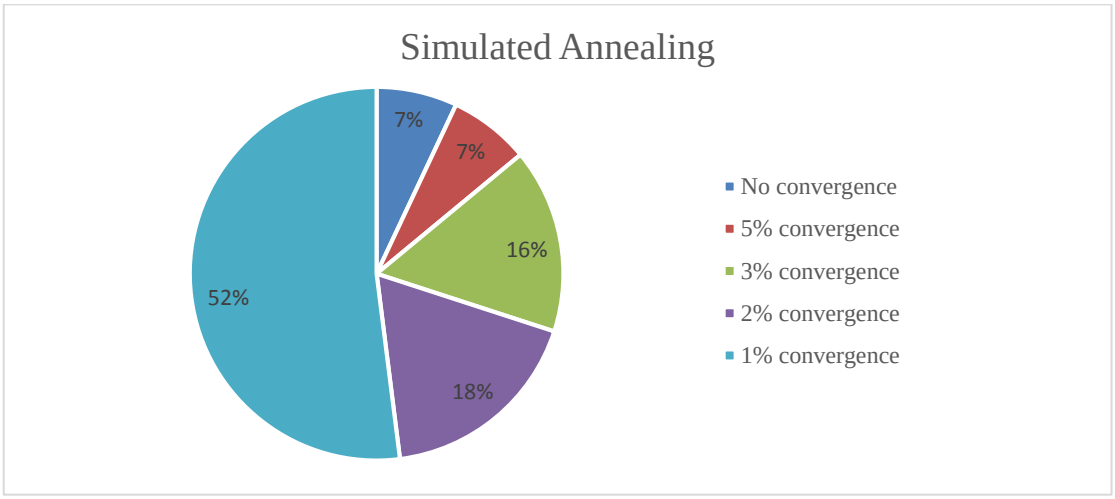

(a) SA algorithm (Literature [24])

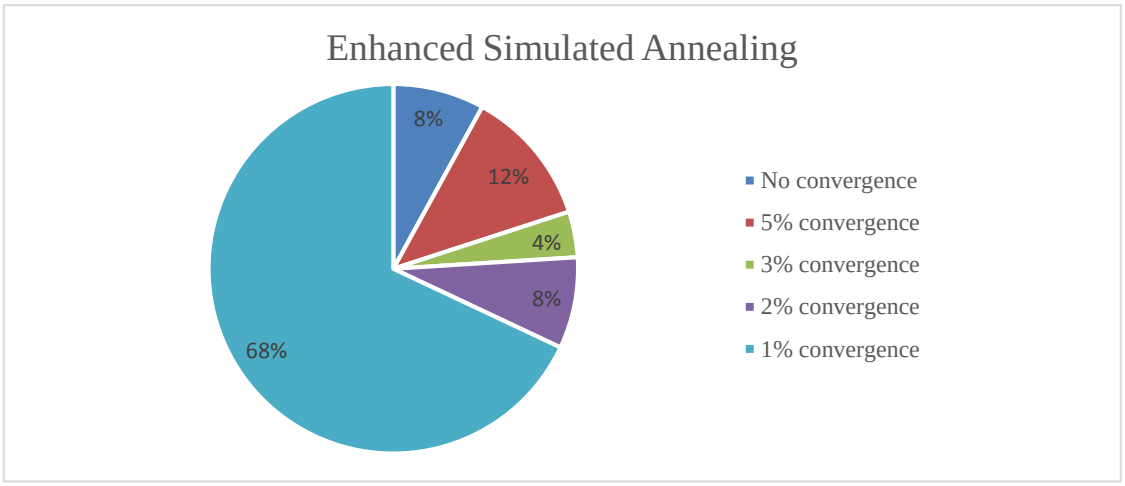

（*b*）ESA algorithm (Literature [25])

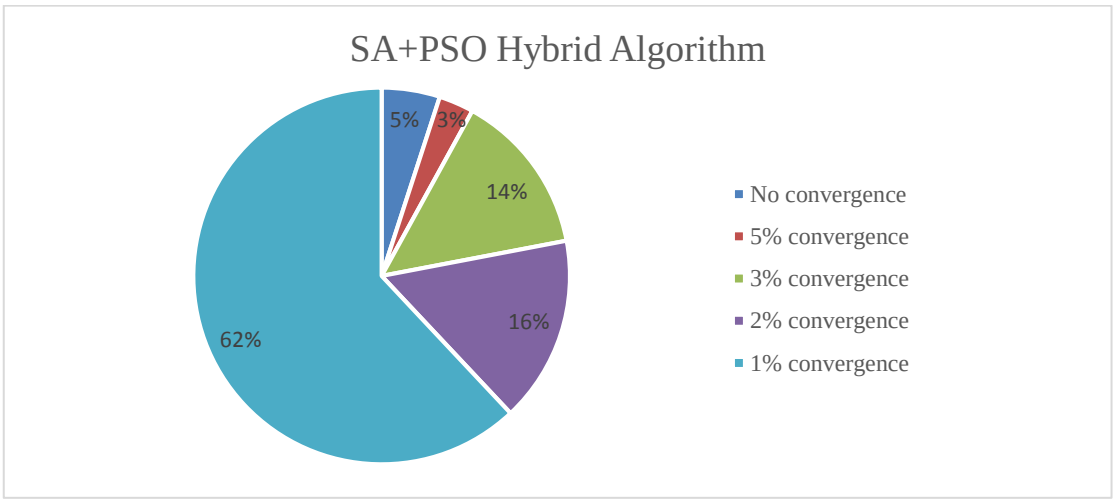

（*c*）SA+PSO mixed algorithm

Figure 3-12 Comparison of convergence accuracy(SA,ESA,SA+PSO)

3.5 Summary of This Chapter

The proposed SA+PSO algorithm in this chapter combines the advantages of PSO algorithm's group diversity and the SA algorithm's progressive convergence advantage. It maintains the balance between global search and local search. It can improve the search efficiency effectively and accelerate the convergence speed of the algorithm. This chapter presents the simulation results of the SA+PSO algorithm. It is verified that the proposed algorithm can track the global maximum power point quickly and accurately through comparing the output power with the characteristics of the photovoltaic panel.When the irradiance changes, it can restart quickly, and the new global maximum power point can be tracked again quickly and accurately. Then the comparison chart between the proposed algorithm and the existing one is given. It can be proved that the algorithm in this thesis has the self-restart ability under the change of the external environment, with higher tracking accuracy and less tracking power oscillation. The tracking speed is faster than existing method. It fully reflects the superiority of the SA+PSO algorithm.

In order to prove the improvement of the tracking performance of the SA+PSO algorithm, this thesis analyzes and simulates the parameters that can improve the performance of the algorithm in next chapter. In particular, the thesis researched the parameters that can improve the algorithm, such as individual and population learning factors, and the number of disturbances Ns, N_T, etc. The thesis analysis and optimization of SA + PSO algorithm in-depth.

4 PARAMETERS OPTIMIZATION AND SIMULATION OF SA+PSO ALGORITHM

Based on the GMPPT algorithm of the SA+PSO mixed method proposed in the previous chapter, this thesis makes a comprehensive analysis of its key parameters. The thesis seeks for an optimized solution again, and improves the algorithm performance further more. As the SA+PSO algorithm flowchart shown in Figure 3-3, the key parameters are the inertia factor w, the individual learning factor c_1 and the population learning factor c_2. Moreover, the other parameters are the starting temperature T_0, the temperature decreasing rate a, and the initial neighbors *step*, the number of disturbances N_S at a given the temperature and neighborhood, the number of neighborhood adjustments N_T at a given temperature, the stop parameter *flag*. Now we analyze them one by one.

4.1 Algorithm Research Considering the Inertia Factor *w*

The selection of inertia weight has a great influence on the algorithm. On one hand, the inertia weight can adjust the influence of the previous search speed on the search speed effectively. On the other hand, inertia weight can balance the relationship between local search and global search effectively. If we select a larger inertia weight, the last search speed will have a large impact on the search speed this time. That is, a large part of the value of $V_i^{(t)}$ will be passed to the next iteration. This will help improve the overall search ability of the algorithm and satisfy the global search ability of the algorithm. When we select the smaller inertia weight, the algorithm inherits less speed from the previous search process. The smaller search speed is favourable for the algorithm to search within the local range. This will improve the local search ability and accelerate the convergence of the algorithm. For existing algorithms, the inertia weight often takes a value that decreases linearly with the number of iterations. Although this method can satisfy the large inertia weight of the algorithm in the early stage and a small inertia weight in the later stage.

However, when the algorithm has already searched for the global maximum in the previous period, the inertia weight cannot reduce quickly and effectively to implement a local search of the algorithm. Because it only adjusts the inertia weight according to the number of iterations, when the algorithm converges to the local optimal value, it cannot jump out of the local optimal value of the algorithm effectively. In order to solve the problem of inertia weight adjustment effectively, this chapter adopts an adaptive algorithm for multi-peak maximum power point tracking. When inertia weight adjusts, the inertia weight changes not only by the number of iterations, but also by the degree of particle aggregation. Its purpose is to balance the local search ability and the global search ability of the algorithm, guarantee the diversity of particles and improve the convergence accuracy of the algorithm.

In the algorithm, the evolutionary state factor δ and the aggregation factor ε are introduced. In the early stage of the algorithm, in order to ensure the particle global search ability, we should select a larger inertia weight avoiding the algorithm falling into the local optimal value and causing the algorithm to be premature. In the later stage of the algorithm, in order to make the algorithm have a better local search capability. To reduce the oscillation of the algorithm near the optimal value, we should select a smaller inertia weight. In order to meet the nonlinear adjustment requirements of inertia weights, we use a strategy of self-adaptive adjustment of inertia weights according to the number of iterations. Then we introduce an evolutionary state factor δ, which represents the relationship between current execution value and the set maximum iteration value of the algorithm. The basic idea is to divide the algorithm into three segments according to the number of iterations. In the first segment, we select a larger inertia weight. In the second segment the inertia weight decreases with the number of iterations nonlinearly. And in the third segment, we selects a smaller inertia weight. Equation 4-1 is a formula for calculating the evolution state factor δ.

$$\delta = exp\left[-30\left(\frac{t}{T}\right)^{s}\right] \tag{4-1}$$

The introduction of the evolutionary state factor δ can satisfy the requirement that the inertia weight has a larger value in the early stage of the algorithm operation and a smaller value in the later stage. However, the inertia weight cannot change significantly when the particle locates near the global optimum position in the early stage of the algorithm operation. In order to make the algorithm more intelligent in the process of running, the particle aggregation factor ε is used to adjust the inertia weight adaptively, and the particle aggregation factor evaluates by the variance of the fitness function value.

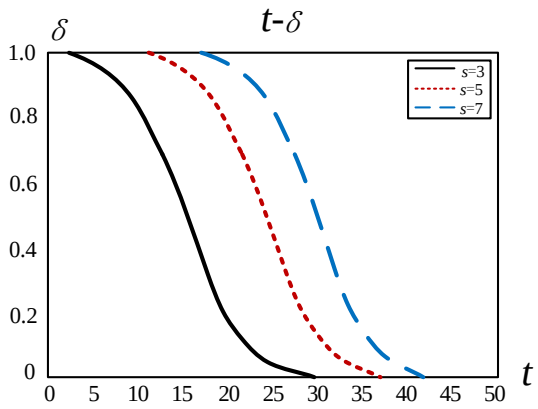

Figure 4-1 Curve of δ

When the particle aggregation factor ε is relatively large, it indicates that the algorithm performs global search at this time, and it needs a larger inertia weight; when the particle aggregation factor ε is relatively small, it indicates that the algorithm is operating a local search at this time. It needs a smaller inertia weights. The following formula gives the calculation of the aggregation factor.

$$f_{avg} = \frac{\sum_{i=1}^{N} f(P_i)}{N} \tag{4-2}$$

$$E = \sum_{i=1}^{N} \left[f(P_i) - f_{avg} \right]^2 \tag{4-3}$$

$$\varepsilon = \sin(\arctan E) \tag{4-4}$$

In the formula, E denotes the variance of the particle fitness function value; $f(P_i)$ denotes the value of the fitness function corresponding to the first particle; f_{avg} denotes the average of the fitness value. When all particles clustered at one point, the position where the particles clustered may not be the global optimal position. In order to make the algorithm jump out of the local optimal position, the anti-aggregation degree factor should adjust for the inertia weight to avoid premature convergence of the algorithm.

In summary, in the adjustment process of the algorithm, the evolutionary state of the algorithm and the degree of aggregation of the particles on the inertia weight should be considered fully. The inertia weight adjusted adaptively according to the evolution state factor and the particle aggregation factor. After the inertia weight processed adaptively, the relationship between the local search and the global search can be balanced. It will satisfy the accuracy requirements of the algorithm. Then the entire particle swarm converges to the

global optimal position of the optimized function quickly, and the function optimization problem can be achieved quickly. The inertia factor should be a function that is first convex upward and then convex downward, so that the algorithm can ensure global search and local fine search at the same time, and the performance of the algorithm will be better.

The adaptive adjustment formula for the inertia weight is shown in Equation 4-5:

$$w = w_{\min} + (w_{\max} - w_{\min}) \times \varepsilon \times \delta + (1 - \varepsilon) \times ws \tag{4-5}$$

In the formula, $w_{\max}$、$w_{\min}$ are the maximum and minimum inertia weights respectively; ws is the value for adjusting inertia weight according to the particle aggregation factor to prevent the algorithm falling into premature. Its value is between 0.08 and 0.15.

4.2 Algorithm Research for Individuals and Population Learning Factors c_1 and c_2

The learning factors include the individual learning factor c_1 and the population learning factor c_2. They represent the case where the particles move to the individual optimal value and the population optimal value. A larger individual learning factor will cause the particles to move to the individual optimal value P_{best} quickly; a larger population learning factor will cause the particles to move toward the population optimal position G_{best} quickly [35]. In order to select different learning factors at different stages of the algorithm operation, we should make nonlinear adjustments to the learning factors. Smaller values allow the particles to linger outside the target area before pulling back; larger values allow the particles to rush toward or over the target area suddenly.

The relationship between c_1 and tracking time can be shown in Figure 4-2:

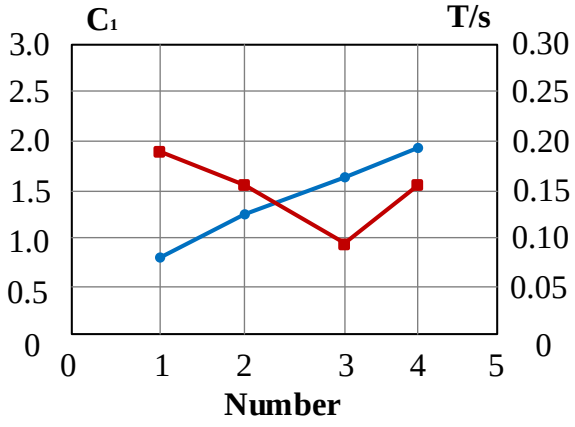

Figure 4-2 Relationship between c_1 and tracking time

When c_1 <1.65, the tracking time reaches the minimum with the increase of c_1 value; when c_1 >1.65, the tracking time increases; when c_1 =0, the global maximum power point cannot be tracked. When c_1 = 0, it means that the particles have no individual cognitive ability and only become a social model with population. It is called global SA+PSO algorithm. Particles have the ability to expand the search space and have a faster convergence speed. However, due to the lack of local search, it is easier for complex problems to fall into the local optimum than the standard algorithm.

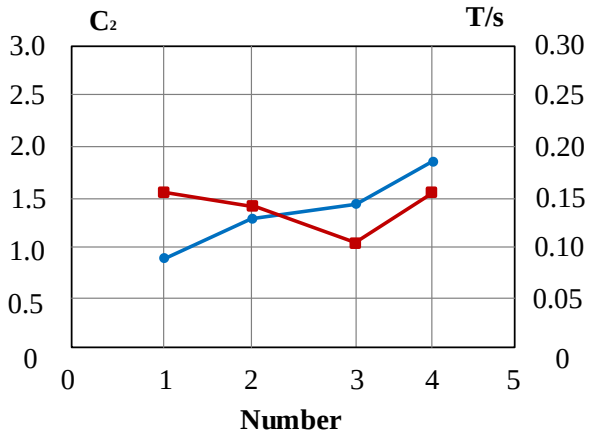

Figure 4-3 Relationship between c_2 and tracking time

The relationship between the population learning factor c_2 and the tracking time can be shown in Figure 4-3. When c_2 < 1.45, the tracking time reaches a minimum as the c_2 value increases; when c_2> 1.45, the tracking time increases; when c_2 = 0, the global maximum power point cannot be tracked. When c_2=0, there is no population information between the particles, and the model becomes a cognitive model only for individuals, which is called a local SA+PSO algorithm. Because there is no information exchange between individual particles, the whole group is equivalent to multiple particles for blind random search. This method has slow convergence rate, so the possibility of obtaining optimal solution is small.

In this algorithm, the first stage of particle search, c_1 takes a larger value, c_2 takes a smaller value; the second stage c_1 takes a smaller value, c_2 takes a larger value. It means that in the first stage, particles should learn more towards their optimal value, accelerate the speed of global search; in the second stage, particles should learn towards global optimal values and enhance local search ability.

4.3 Algorithm Research When Considering Number of Particles and Maximum Speed

The selection of the maximum particle speed affects not only the particle's convergence rate, but also the convergence accuracy. When the maximum speed value is large, it will be beneficial to the fast convergence of the algorithm. However, due to the large maximum speed, the particle can have a large span, and it is easy for the particle to cross the global optimal position and the optimal solution cannot obtain. The smaller maximum speed can make the algorithm converge to the optimal solution. However, because the particle's spanning degree is small, the global search ability of the algorithm reduces. And the algorithm often converges to the local optimal solution. When the maximum speed is selected to be small, it is not conducive to the rapid convergence of the algorithm.

In addition, the number of particles is also a key element that affects the convergence speed of this algorithm [36]. If the setting is small, the search speed will be fast, but the final extremum of the searched power will not fall to the maximum value necessarily; if the setting is large, the global optimal value can be found easily, but the algorithm convergence speed will reduce greatly. It will lose the advantage of the algorithm. According to a large number of experiments, combined with the convergence of subsequent algorithms, this thesis limits the maximum number of iterations to 6. In a 3×1 PV array, the number of particles is set to 3 as the best. At this moment the convergence speed and tracking accuracy are ideal.

4.4 Algorithm Research Considering T_0, a and *step*

The initial temperature mainly affects the size of the optimal solution acceptance probability. If the temperature is higher, then P_r is larger (of course when P_k is smaller than P_i). The possibility of accepting the reduced power point as a new operating point increase. In this way, the probability of the algorithm traversing several peak intervals of the power voltage curve increases. Therefore, the probability of tracking the global maximum power point also increases correspondingly, that is, the reliability of the algorithm increases. However, if T_0 is too high, the time required cooling to a certain temperature is too long. It increases the time for the algorithm to track the maximum power point and slows down the tracking speed. The algorithm optimization reference [21] proposed that the simulated annealing method can combine with other algorithms. Other algorithms provide the initial value for

disturbance. One of the most intuitive applications is to assign the initial value obtained by PSO algorithm to the simulated annealing algorithm. In this case, since the initial value is closer to the optimal point, the initial temperature T_0 can reduce properly. It increases the tracking speed, and does not affect the overall reliability of the algorithm at the same time. In this way, the algorithm is system dependent, because empirical methods need to know the number of parallel photovoltaic panels to determine the disturbance voltage interval.

The temperature drop rate affects the temperature of the algorithm directly. Therefore, the effect of the temperature drop rate on the algorithm can refer to the influence of temperature on the algorithm. Of course, this factor is also a contradiction between the reliability and the tracking speed. If the temperature decreasing speed a is smaller, the temperature drops faster, the reliability is lower, the tracking speed is faster; and vice versa, if the temperature decreasing speed a is greater , the temperature drop slower, reliability is higher and the tracking speed is slower.

In the SA+PSO mixed algorithm proposed in this thesis, the value of the initial neighborhood has adjusted adaptively. Therefore, the selection range of the initial neighborhood is more flexible. This value will reach a more appropriate, ideal and feasible value after several adjustments.

4.5 Algorithm Research Considering N_S and N_T

If there are more disturbances in a certain neighborhood, the probability of traversing all the peak intervals in this neighborhood is higher. It means that the probability of tracking the maximum power point in this neighborhood is higher. At the same time, it is obvious that if the number of disturbances is greater, the longer time the algorithm takes, the slower it is to track the maximum power point [42]. This is also a contradiction between reliability and tracking speed. The current algorithm uses a fixed number of disturbances N_S, and does not change the value of the number of disturbances for changes in the size of the neighborhood. However, in fact, if the neighborhood is smaller, then the required number of disturbances is smaller, and vice versa. Therefore, the further improvement is that the number of disturbances can adjust adaptively with the size of the neighborhood, and the number of disturbances in the neighborhood hours can reduce to increase the tracking speed. When the neighborhood is large, the number of disturbances can increase to improve the reliability of the algorithm.

For N_S parameters, we do a simulation experiment in MATLAB/Simulink. Among them, N_S is from 1 to 10. Each N_S performs five experiments. And 50 simulation results are obtained totally. The maximum power point tracking accuracy of the simulation results and the time required for the tracking of the algorithm are listed as a line chart. It represents the changes visually in the performance of the algorithm brought about changes in the N_S, as shown in figure 4-4.

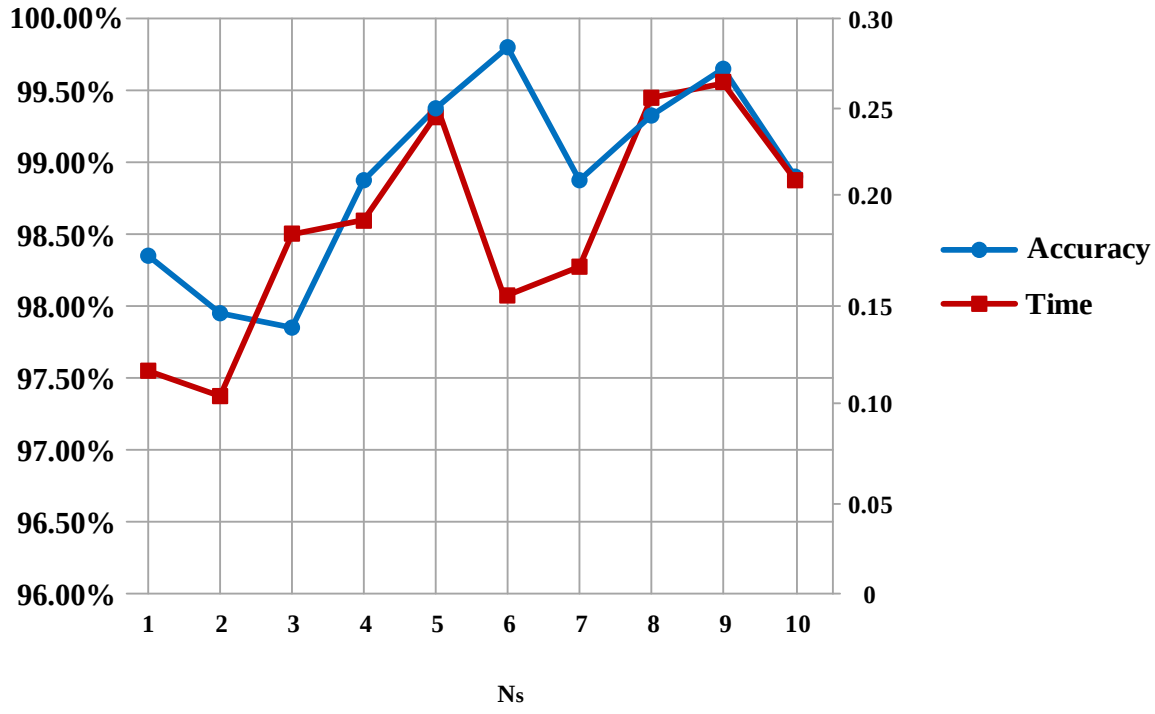

Figure 4-4 Chart of N_S and Tracking Accuracy

From Figure 4-4, we can see that with the increase of the number of disturbances at a given temperature and neighborhood N_S, the tracking accuracy of the algorithm is improved. Nevertheless, the corresponding tracking time is longer, reflecting the contradiction between tracking accuracy and tracking speed. This result is consistent with our previous analysis and predictions.

A possible improvement is to change the N_S as the neighborhood changes adaptively. When the neighborhood is small, there is no need to disturb too many times the output voltage. We can reduce the N_S and increase the tracking convergence speed. When the neighborhood is large, too few disturbances do not traverse the regions where the power peak is located easily. It may reduce the reliability of algorithm, so it is necessary to increase N_S at this time to increase the probability of global maximum power point tracking.

Similar analysis with N_S, we can get a similar inference: the greater the number of neighborhood adjustment N_T, the higher the reliability, the slower the tracking speed. It is also a contradiction between tracking accuracy and tracking speed. What needs to be discussed further is how to make the N_T self-adaptive adjustment better, so that N_T should be increased when the number of adjustments should be increased to improve reliability. N_T should reduce and the tracking speed should increase when the number of adjustments reduce.

For N_T parameters, we do 50 simulations in MATLAB/Simulink. Among them, N_T is from 1 to 5. Each N_T does 10 experiments. And total 50 simulation results are obtained. The simulation results for each N_T are averaged. Then the maximum power point tracking accuracy of the simulation result and the time required for the tracking of the algorithm are listed as a line chart. It represent changes in the performance of the algorithm brought about by changes in the N_T visually, as shown in figure 4-5.

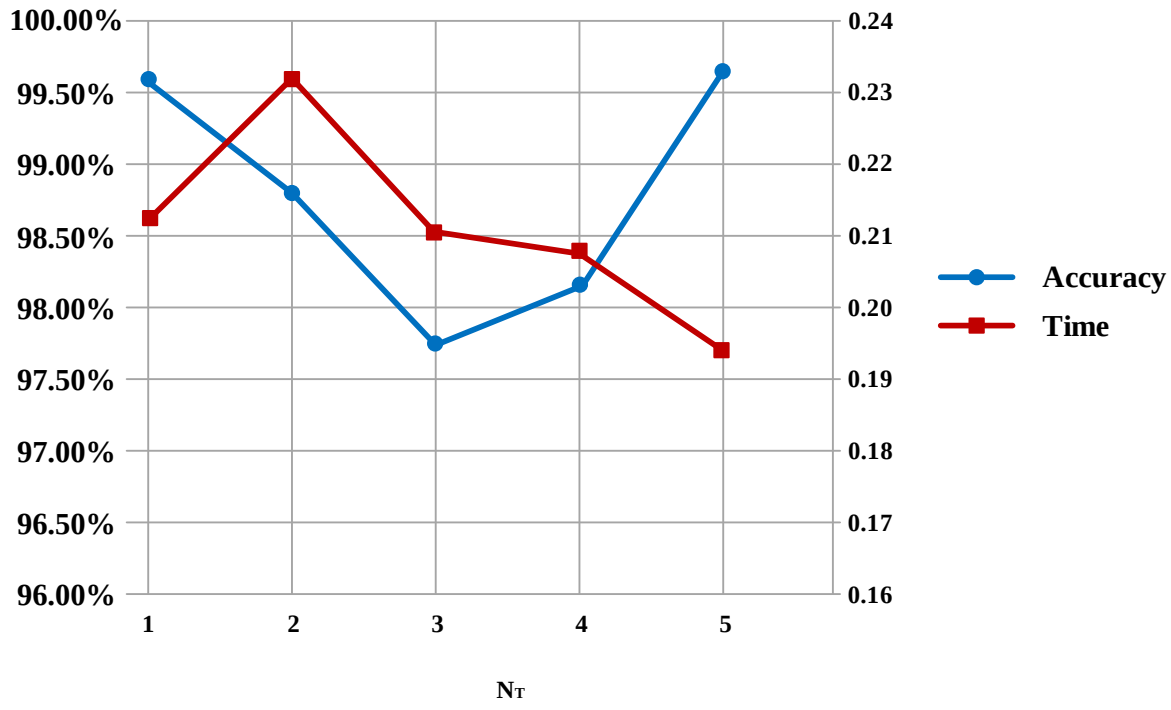

Figure 4-5 Chart of N_T and Tracking Accuracy

According to the analysis and prediction of N_T parameter above, the performance of the algorithm should have the following changes with the increase of N_T: the tracking accuracy is higher, but the tracking speed reduces. However, from the simulation results, there is no

approximate linear effect of NT on the tracking accuracy and tracking time. For this deviation, we still need further analysis and discussion.

4.6 Algorithm Research Considering Stop Parameters *flag*

The stop parameter *flag* is that the output power of successive *flag* times is very close to the stored maximum power point power. At this moment, we can assume that the algorithm has tracked the global maximum power point [43]. If the flag is greater, then the more recorded operating points close to the stored global maximum power, the higher the probability that the algorithm has tracked the global maximum power point. However, *flag* does not need to take a large value, which will increase the algorithm convergence time. Simulation experiments show that when the *flag* value exceeds 3, the reliability of the algorithm has little effect. Therefore, we choose flag as 3, and there is no need to make too many changes and discussions on this parameter.

4.7 Summary of This Chapter

This chapter analyzes the key parameters of the SA+PSO mixed algorithm. Theoretically, the impact of various key parameters on the performance of the algorithm is specified and predicted. At the same time, statistical experiments are carried out for parameters, such as inertia factor w, individual learning factor c_1 and population learning factor c_2, and N_S, N_T. Then the thesis gives the idea for further improving the performance of the algorithm. the thesis also performed a simple analysis for parameters that did not have space improvement.

5 EXPERIMENTAL PLATFORM CONSTRUCTION AND EXPERIMENTAL RESULTS ANALYSIS

In this chapter, hardware experiment performed for the proposed SA+PSO mixed algorithm verification in the above chapters. The purpose is to implement the global maximum power point tracking for multi-peak conditions. The thesis presents from the design of photovoltaic analog sources, the selection of experimental components, and the boost circuit design.

5.1 Experimental System Solution

5.1.1 Photovoltaic Analog Source Design

The photovoltaic optimization module based on the SA+PSO mixed algorithm and a multi-peak problem require a photovoltaic submodule, i.e. a photovoltaic analog source is needed. Due to laboratory conditions limited, the DC voltage source and resistance are used to simulate the photovoltaic submodules, as shown in Figure 5-1.

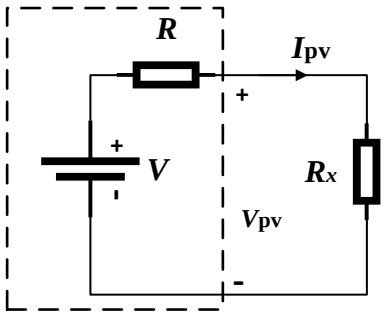

Figure 5-1 DC source and resistance simulate PV submodule schematic diagram

The DC voltage source always operates in the constant voltage output mode. The series power resistor is *R* and the output voltage value is *V*. Thus, the simulated power-voltage relationship of the photovoltaic submodule can express as:

$$P_{\mathrm{PV}} = -\frac{1}{R}\left(V_{\mathrm{PV}} - \frac{V}{2}\right)^2 + \frac{V^2}{4R} \tag{5-1}$$

The relationship between current and voltage is:

$$I_{\mathrm{PV}} = \frac{1}{R}(V - V_{\mathrm{PV}}) \tag{5-2}$$

So the voltage, current and power at the maximum power point are:

$$V_{\mathrm{mpp}} = \frac{V}{2}, \quad I_{\mathrm{mpp}} = \frac{I_{\mathrm{sc}}}{2} = \frac{V}{2R}, \quad P_{\mathrm{mpp}} = \frac{V^2}{4R} \tag{5-3}$$

The PV curves and IV curves are shown in Figure 5-2. It can be seen from Figure 5-2 that the simulated PV curve is a symmetrical single-peak curve. The voltage value of the DC source and the series power resistance can be changed. We can also change the position and power of the maximum power point. The structure of this DC source and resistor can only simulate the single-peak photovoltaic characteristic curve, and the verification of the photovoltaic optimal power control algorithm based on the SA+PSO needs to simulate the PV array with multi-peak output characteristics. Therefore, we use Chroma PV simulator (model 62150H-1000S) to realize multi-peak PV array simulation. The load used in the experiment is an electronic load (model IT8512). It can choose constant voltage, constant current, or constant resistance mode that used to absorb power.

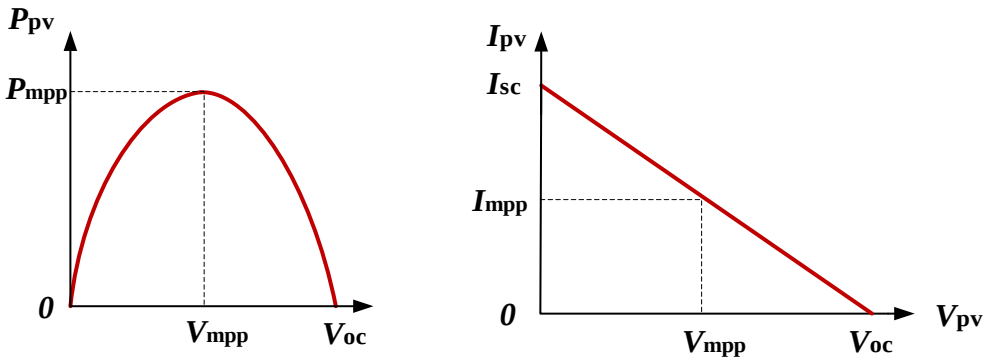

(a) P-V curve (b) I-V curve

Figure 5-2 P-V and I-V characteristic curves of simulated PV submodules

5.1.2 DSP Selection

TMS320F28335 digital signal processor is TMS320C28X series of floating-point DSP controller. The device has high precision, low cost, low power consumption, high performance, high degree of peripheral integration, large storage of data and programs, and more accurate A/D conversion [19].

TMS320F28335 has 150MHz high-speed processing capability, 32-bit floating point processing unit, 6 DMA channels to support ADC, McBSP, and EMIF. There are up to 18

PWM outputs, among which 6 channels are TI unique high-precision PWM output. (HRPWM), 12-bit 16-channel ADC [40]. Using its floating-point arithmetic unit, it can write control algorithms quickly without spending too much time and effort on decimal operations. Compared with previous generation DSPs, the average performance is improved by 50% and is compatible with fixed-point C28x controller software. Simplify software development, shorten development cycles, and reduce development costs.

(1) The algorithm can be calculated and controlled quickly: the Harvard bus architecture makes data and instruction access faster. CPU has an 8-stage pipeline, and the built-in hardware multiplier can perform fixed-point operations.

(2) The global maximum power point tracking method required fast and real-time sampling of the voltage and current at both ends of the photovoltaic cell. Two sample holders enable the AD converter to be sampled sequentially. The sequencer allows multiple conversions of the same channel multiple times.

(3) PWM signal used to drive the switch of the DC-DC converter on and off: Two EV event management modules, 3 comparison units of each EV can generate 6 dead-band programmable PWM signals, two universal timer can also generate two PWM signals.

5.1.3 Boost Circuit Design

DC-DC converters convert direct current into another type of controllable direct current. In photovoltaic power generation systems, DC-DC converters are used mainly to receive control signals for maximum power point tracking. There are many types of DC-DC converters, the more common ones are: Buck Converters, Boost Converters, and Buck-Boost Converters (CUK Converters) [41]. The experimental platform built in this thesis is a Boost converter. The schematic diagram of the circuit is shown in Figure 5-2.

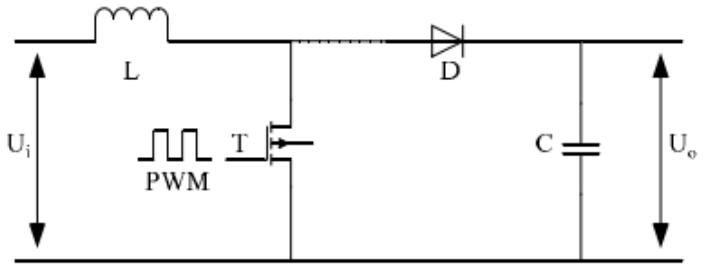

Figure 5-3 Boost circuit schematic

The Boost circuit design structure is shown in Figure 5-4. Since the Boost circuit has only one switching device, a single driver chip is used. The DSP driving signal which DSP exploitation board output is separated into a single driver chip after optocoupler isolation, the output drive signal drive MOSFET. Vin+, Vin-, Vout+, Vout- are the inputs of the Boost circuit and the load. Boost converter input voltage sampling voltage Hall sensor selection, inductor current sampling selection of current Hall sensor. The voltage and current signals are input into the DSP exploitation board via the interface to perform dual-loop voltage-current control and MPPT algorithm after sampling and conditioning. The designed Boost circuit can be used as a converter to connect the PV array with the load simultaneously for the GMPPT algorithm experiment based on the SA+PSO mixed algorithm.

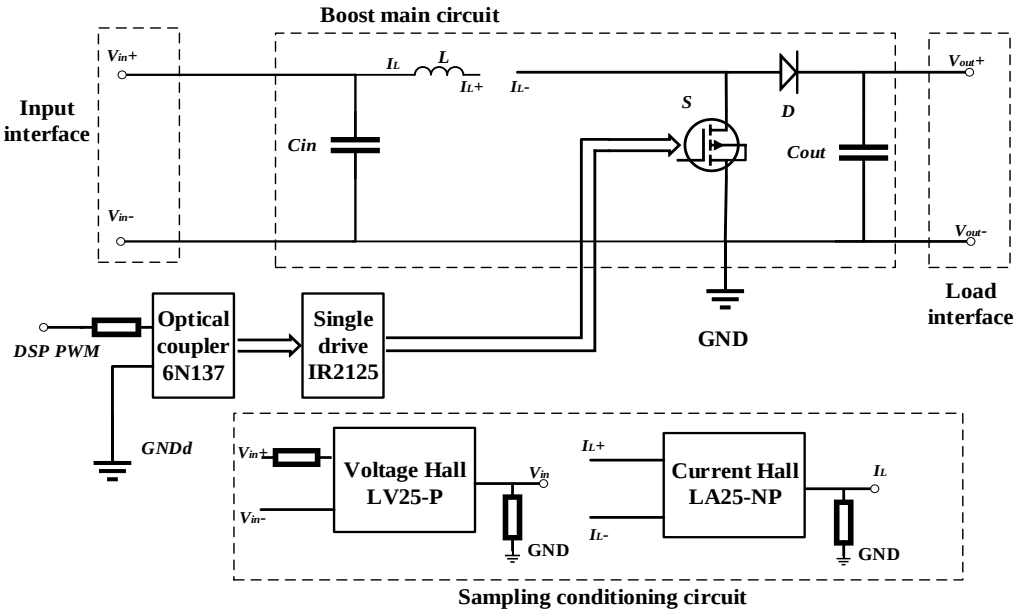

Figure 5-4 Boost converter design

5.2 Experimental Device Selection and Circuit Design

Referring to the parameter design and simulation parameters in the previous chapters, the model and related parameters of the experimental components finally determined in this section are as follows:

Table 5-1 Component Selection and Specifications

Components	Selection	Standard
Half bridge driver chip	IR2184	15Vdriving
Single driver chip	IR2125	15Vdriving
MOSFET	IPP075N15N3G	150V/100A
Operational Amplifier	TL084/TL082	Integrated Amplifier 4/2
Voltage Hall Sensor	LV25-P	-
Current Hall Sensor	LA25-NP	-
Inductor L	-	1mH
Inductor L_1,L_2	-	350μH
Capacitor C_{in},C_{out}	-	470μF
Capacitor C_1,C_2,C_3	-	470μF

The main circuit diagram of the experiment is shown in Figure 5-5. The actual circuit diagram is drawn by Matlab/Simulink. According to the principle of flowchart in Figure 5-4, each component is assigned specifically and the following circuit diagram is obtained. The green part of the circuit diagram is input and output.

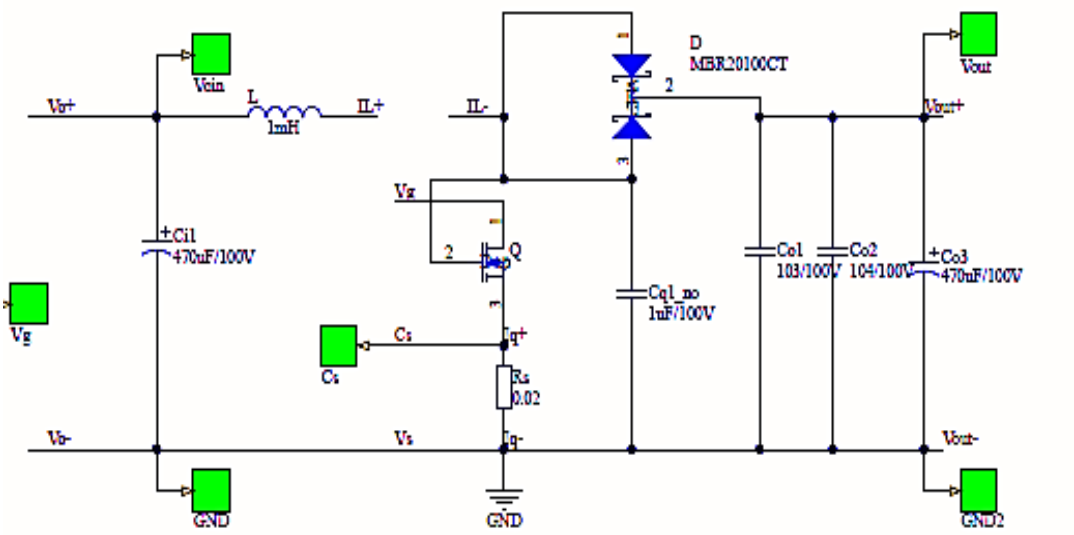

Figure 5-5 The main circuit diagram of the hardware experiment

It is also the data that needs attention in this experiment. It mainly focuses on whether the output voltage of the circuit is close to the voltage on the ideal characteristic curve of the photovoltaic panel. When it is determined that the two voltages are the same, it can be determined that the output of the photovoltaic panel is above the maximum power point.

The final Boost circuit board manufactured and debugged is shown in Figure 5-6. The two dark blue parts in the figure are the current and voltage Halls. The yellow wire is connected in series with a coil. The black components are capacitors. In the process of making a circuit board, in order to ensure the accuracy of important detection points, several detection points can be set to be compared, which can also improve the accuracy of the experimental results.

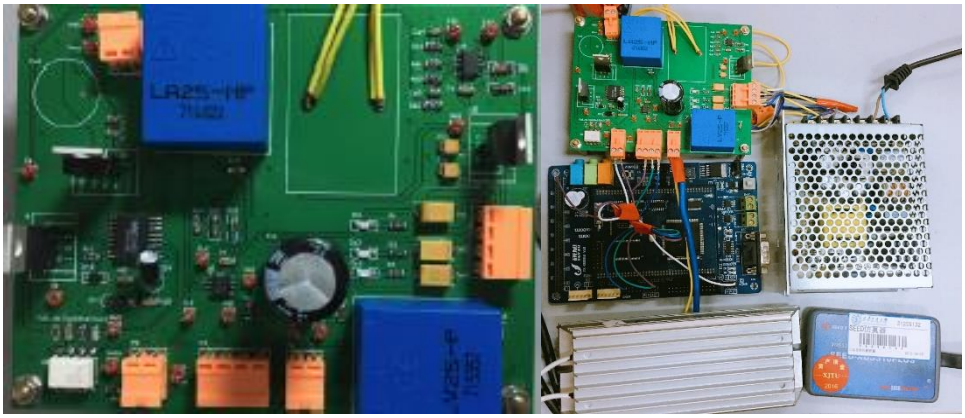

Figure 5-6 Boost circuit board diagram and test bench setup

After ensuring that several debuggings of the Boost circuit board are accurate, this thesis will perform the hardware experiment of the SA+PSO algorithm in the next section.

5.3 Analysis of Experimental Results

5.3.1 Experiment Platform Based on SA+PSO Algorithm

This thesis uses the Chroma PV Simulator (model 62150H-1000S) to simulate the presence of a multi-peak PV array during the experiment. The Boost circuit acts as a DC-DC converter and the electronic load operates in constant resistance mode. The experimental bench is shown in Figure 5-6.

Figure 5-7 SA+PSO mixed algorithm hardware experiment platform

In order to verify the proposed GMPPT method based on SA+PSO mixed algorithm, three sets of experiments are conducted in this thesis for photovoltaic panels with full illumination and PV arrays with multiple peak shielding conditions.

5.3.2 Experiment Results Based on SA+PSO Mixed Algorithm

The first set of experiments: The input of the Boost circuit is a photovoltaic panel without multi-peaks. Its output power-voltage curve exhibits a single-peak characteristic with a maximum power point voltage of 15V and a maximum power point power of 28.7W. The experimental waveform of the photovoltaic panel output voltage is shown in Figure 5-8.

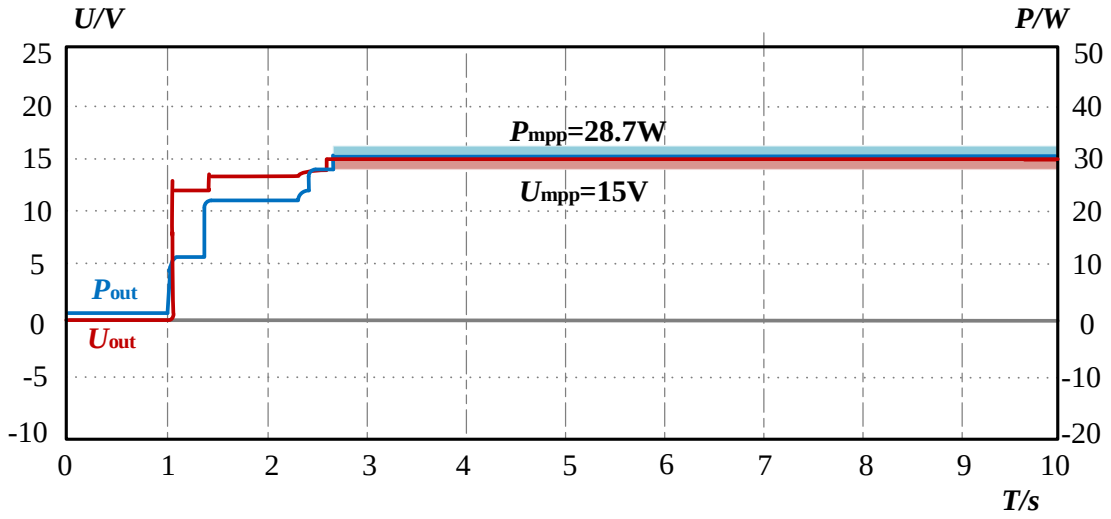

Figure 5-8 Single Peak Test PV Array Output Voltage Waveform

During the tracking process, the photovoltaic panel output voltage is disturbed randomly and stabilized eventually at the maximum power point voltage of 15V, i.e. the maximum power point is tracked.

The second set of experiments: The input of the Boost circuit is a photovoltaic array with an occlusion phenomenon.

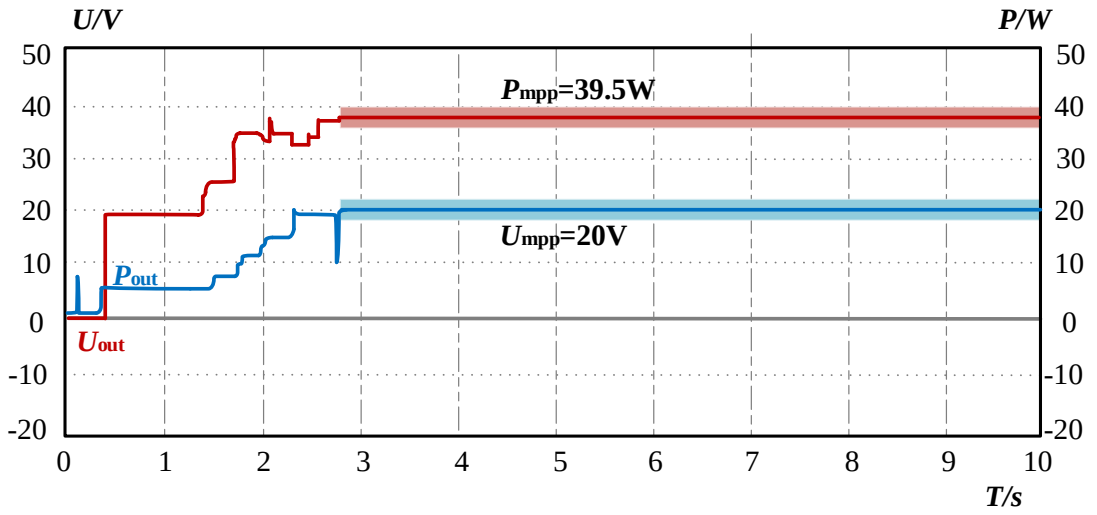

Figure 5-9 Double-peak experimental PV array output voltage waveform

Its output P-V characteristic curve exhibits double-peak characteristics. The global maximum power is 39.5 W, and the maximum power point voltage is 20V. The experimental waveforms of the output voltage and output power of the photovoltaic panel are shown in Figure 5-9.

During the tracking process, the photovoltaic panel output voltage is randomly disturbed and eventually stabilized at the maximum power point voltage of 20V. At this time, it is determined that the maximum power point is tracked.

The third group of experiments: The input of the Boost circuit is a photovoltaic array with an occlusion phenomenon. The input is a 3×2 photovoltaic array. Its output P-V characteristic curve exhibits a multi-peak characteristic, as shown in Figure 5-10. The value on the left side of the photovoltaic panel in the figure represents the light (in W/m^2) it receives. It can be seen that this is a photovoltaic array with multiple peaks.

The global maximum power is 51W and the maximum power point voltage is 34V.

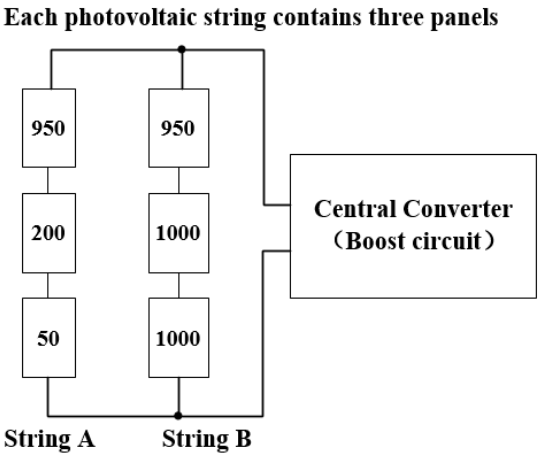

Figure 5-10 Misaligned PV array structure

The output power of the PV array - voltage P-V curve and current - voltage I-V curve are shown in Figure 5-11.

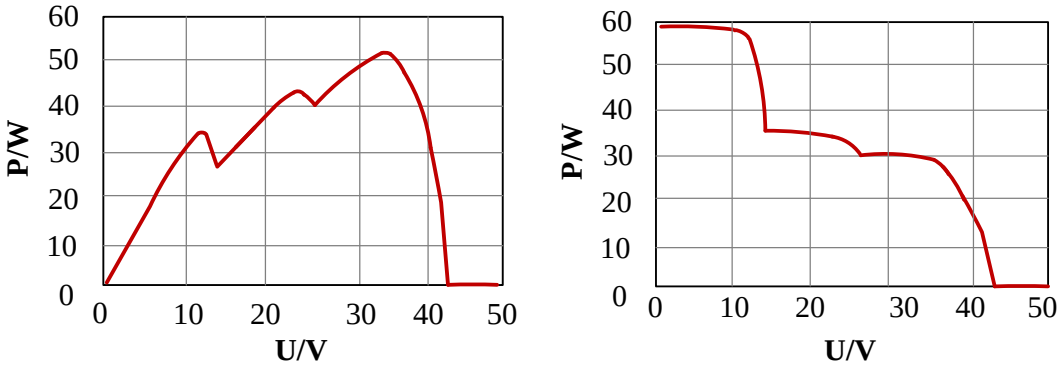

(a) PV array P-V curve (b) PV array I-V curve

Figure 5-11 PV array P-V and I-V characteristics

The experimental waveform of PV array output voltage and power is shown in Figure 5-12. During the tracking process, the output voltage is randomly disturbed and eventually stabilized at the maximum power point voltage of 34 V and the maximum power of 51 W. It means the global maximum power point is tracked.

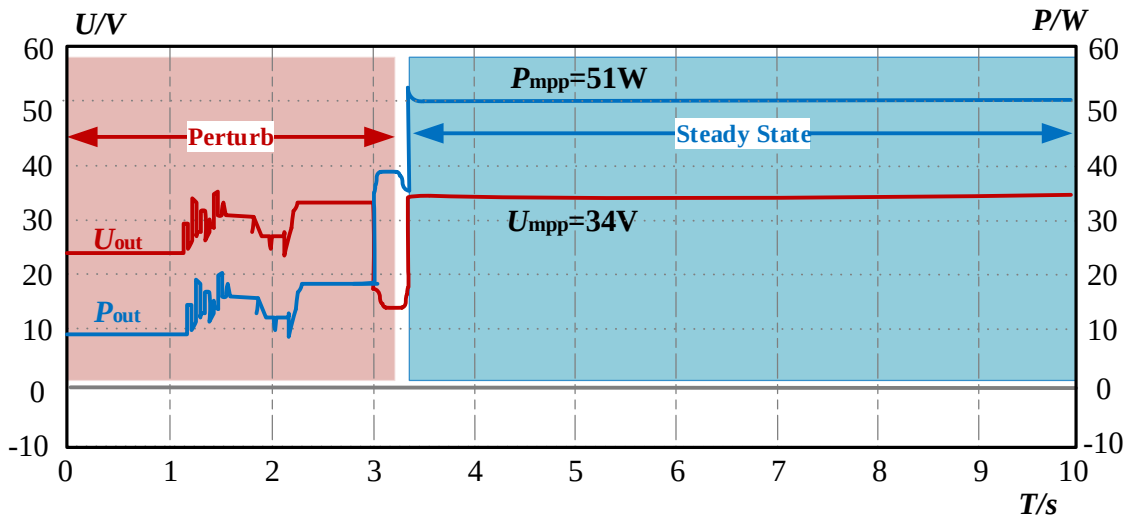

Figure 5-12 Multi-peak experimental PV array output voltage and power waveform

From the above experimental results, the global maximum power point tracking method based on the SA+PSO mixed algorithm can track the global maximum power point of the PV array accurately and quickly under any multi-peak conditions, and the steady-state oscillation is small.

5.4 Summary of This Chapter

This chapter introduces the experimental program, including the realization of photovoltaic analog sources and loads, the design of the converter, etc. We list the types and specifications of the main experimental devices and set up an experimental platform. Finally, we analyse the experimental results. In this chapter, experiments operate using SA+PSO algorithm GMPPT method under single-peak and multi-peak conditions. It can be concluded that the SA+PSO algorithm GMPPT method can track the global maximum power point of the PV array accurately and quickly under any multi-peak conditions.

6 CONCLUSION

6.1 Conclusion

This thesis compares the existing artificial intelligence global maximum power point tracking method under multi-peak conditions, focusing on the algorithms based on particle swarm optimization, simulated annealing and other algorithms. Then a mixed global maximum power point tracking method based on SA+PSO algorithm is proposed. In this thesis, the proposed algorithm is simulated under single-peak, multi-peak and irradiance changing conditions. All the parameters in the algorithm are optimized. Finally, through the establishment of a hardware experiment platform, the research results are verified and summarized. This thesis obtained the following conclusions in the research process:

(1) This thesis compares the existing GMPPT algorithm under single and multiple peaks at internal and abroad to analyze existing problems and deficiencies. This thesis outlines the physical model and simplified mathematical model of photovoltaic cells. According to the basic principles of photovoltaic cells, the external characteristics of photovoltaic cells under the changes of temperature and light irradiance are analyzed. This thesis summarizes the principle and process of maximum power point tracking method, aims at multi-peak optimization algorithms such as traditional disturbance observation methods and artificial intelligence algorithms. This thesis simulates the power characteristics of the algorithm under environmental changes and complex lighting conditions in Matlab/Simulink. .

(2) This thesis proposes a global maximum power point tracking method based on the simulated annealing and particle swarm optimization mixed algorithm. This algorithm combines the advantages of PSO algorithm's population diversity and the SA algorithm’s progressive convergence, keeping the balance of the global search and local search so that can improve the search efficiency of the algorithm efficiently. The proposed algorithm has self-restart ability to deal with sudden changes in the environment, more appropriate termination conditions and adaptive adjustment mechanisms in the neighbourhood. The tracking accuracy is improved, the convergence speed is increased, and the oscillation is reduced. In order to verify the accuracy of the proposed SA+PSO mixed algorithm, this

thesis compares the SA+PSO mixed algorithm with the SA algorithm and the ESA algorithm for 50 simulations. Then it obtains two comparative graphs of the tracking time and the tracking accuracy. The SA+PSO mixed algorithm is robust verifying from the graph. Compared with the existing algorithms, the SA+PSO mixed algorithm can achieve tracking accuracy of 95%. The proposed algorithm can track the global maximum power point with high speed, high accuracy and less time.

(3) In this thesis, each parameter in the SA+PSO mixed algorithm is researched in detail and depth. The influence of each key parameter on the performance of the algorithm is specified and predicted. For the parameters that have improved space, such as inertia factor w, individual learning factor c_1 and population learning factor c_2, N_S and N_T disturbances, statistical experiments are conducted, and the ideas for further improving the performance of the algorithm are given. A simple analysis is also performed for parameters that does not need improvement. Finally, the parameters in the SA+PSO mixed algorithm are satisfied to optimize the use of the algorithm.

(4) This thesis builds a hardware circuit based on software simulation. Under single-peak and multi-peak conditions, hardware experiments are operated to verify the feasibility of the SA+PSO mixed algorithm, from the specific experimental device selection to hardware test platform debugging. The SA+PSO mixed algorithm is verified for its ability to track GMPP in different situations. This thesis sets up the MPPT experiment platform of photovoltaic power generation system, introduces the structure of experimental platform. This thesis analyzes the structure and parameters of boost circuit in detail. This thesis designs a control circuit suitable for this algorithm, and configures the control circuit with DSP as the core, which includes sampling circuit, signal conditioning circuit, drive circuit, buffer protection circuit and other peripheral circuit component parameters. The experimental results show that the system operates stably at the maximum power point voltage through the output voltage of the photovoltaic panel under single peak conditions. Under the multi-peak conditions, the output voltage and current of the photovoltaic panel are reduced a bit. The photovoltaic panel is operated under the control system to re-stabilize the voltage output at the maximum power point under multi-peak conditions. It shows that the proposed algorithm in this thesis runs stably on the hardware circuit and has better response to changes in the environment. So far, this thesis has completed all experiments on the proposed SA+PSO mixed algorithm.

6.2 Prospect

This thesis does some work on the SA+PSO mixed algorithm global maximum power point tracking method under multi-peak conditions. However, due to limited time, the work of this thesis has many imperfections. The prospect for follow-up scientific research is as follows:

(1) The proposed SA+PSO mixed algorithm can still improve. For example, the conversion efficiency of photovoltaic modules in the industrial market can reach 99.9%. However, the efficiency of the algorithm in the thesis still needs to be improved.

(2) In this thesis, 50 experiments are operated to verify the SA+PSO mixed algorithm. In practice, more and more experimental data need for reference. The more experiments, the greater the accuracy.

(3) The next step of research should be to study other more artificial intelligence algorithms. Each algorithm has its advantages, such as fuzzy control, BP neural algorithm, etc. It should try more combination methods to achieve more. The purpose of tracking the global maximum power point is more accurate and faster.

(4) The efficiency of photovoltaic modules is not only related to the GMPPT algorithm. In the future, research on photovoltaics should carry out more on software algorithms and hardware topology at the same time.

7 REFERENCES

[1] Chen Dongpo. Review and Prospect of China's Photovoltaic Market in 2017-2018[J]. *Electronic Products World*, 2018, 25(04): 11-13.

[2] Ruan Xiaowei. Research on the Influence of Photovoltaic Power Generation on Power System[J]. *Engineering Construction and Design*, 2018(06):50-51.

[3] Hu Yunyan, Zhang Ruiying, Wang Jun. Development Status and Prospects of Solar Photovoltaic Power Generation in China [J]. *Journal of Hebei University of Science and Technology*, 2014, 35(01): 69-72.

[4] Shi Dan. Improvement of energy efficiency in the process of economic growth in China [J]. *Economic Research*, 2002(09):49-56+94.

[5] Ding Ming, Wang Weisheng, Wang Xiuli et al. Review of large-scale photovoltaic power generation impact on power system[J]. *Proceedings of the CSEE*, 2014, 34(01): 1-14.

[6] Li Yong, Cheng Hanxiang, Chen Xingcan et al. Photovoltaic cell output characteristics and maximum power tracking [J]. *Journal of North China Electric Power University* (*Natural Science*), 2017, 44(01): 70-75.

[7] Cui Yan, Cai Binghuang, Li Dayong et al. Comparative study of MPPT control algorithms for solar photovoltaic systems [J]. *Chinese Journal of Solar Energy*, 2006(06):535-539.

[8] Rong Desheng, Liu Feng. Research on Improved Disturbance Observation Method in Photovoltaic MPPT[J]. *Journal of Electric Power Systems and Automation*, 2017, 29(03): 104-109.

[9] Liu Mingliang, Zhang Yi, Fan Yuanliang et al. An Adaptive MPPT Control Strategy Based on Variable Step Conductance Increment Method [J]. *Renewable Energy*, 2017, 35(05): 681-688.

[10] Jing Hongli, Zhao Peng. MPPT design of photovoltaic power generation system based on fuzzy control[J]. *Foreign Electronic Measurement Technology*, 2016, 35(01):80-83.

[11] Liu Jianhui, Li Bo. Research on MPPT based on genetic ant colony algorithm under local shadow [J]. *Renewable Energy*, 2017, 35(01): 13-19.

[12] Zhu Yanwei, Shi Xinchun, Dan Yangqing et al. Application of particle swarm optimization algorithm in multi-peak maximum power point tracking of photovoltaic

arrays[J]. *Proceedings of the CSEE*, 2012, 32(04): 42-48+20 .

[13] Li Shanshou. Mismatch analysis and optimal control of photovoltaic systems under shadow conditions [D]. *Hefei University of Technology*, 2016.

[14] Li Shanshou, Zhang Xing, Zhang Hongxuan et al. Global MPPT method based on power closed-loop control and PSO algorithm[J]. *Proceedings of the CSEE*, 2014, 34(28):4809-4816.

[15] Zhou Hang. Research on MPPT control of partial shaded photovoltaic power generation system based on particle swarm optimization [D]. *Tianjin University*, 2009.

[16] Zheng Junguan, Wang Shuojun, Qisaisai. Application of Improved Particle Swarm Optimization Algorithm in Multi-peak Photovoltaic MPPT[J]. *Electric Power & Energy Management Technology*, 2018(06): 53-59.

[17] Yang Jie, Jiang Lin, Mou Qingping. Photovoltaic multi-peak maximum power tracking algorithm based on simulated annealing particle swarm optimization[J]. *Journal of Computer Applications*, 2014, 34(S1): 330-333.

[18] Xu Dehong, Ma Wei, Wang Yusheng. Power Electronics Technology [M]. *Beijing: Science Press*, 2006.

[19] Ning Gai, Zeng Xiangjun, Luo Yiping. DSP controller principle and application [M]. *Beijing: Science Press*, 2009, 151-198D.

[20] Divya, A. Karthikeyan, G. Panneerselvam, et al, "A maximum powerpoint tracking using perturb and observation algorithm by LABVIEW and arduino," *2014 International Conference on Science Engineering and Management Research (ICSEMR)*, Chennai, 2014, pp. 1-4.

[21] S. Qin, M. Wang, T. Chen , et al, "Comparative analysis of incremental conductance and perturb and observation methods to implement MPPT in photovoltaic system," *International Conference on Electrical and Control Engineering*, Yichang, 2011, pp. 5792-5795.

[22] G. Chujia, Z. Aimin, Z. Hang, et al, "A fuzzy MPPT method for PV array in power system," *The 27th Chinese Control and Decision Conference* (CCDC), Qingdao, 2015, pp. 5085-5089.

[23] Y. Zheng, W. Wang, W. Chen, et al, "Research on MPPT of photovoltaic system based on PSO under partial shading condition," *35th Chinese Control Conference* (CCC), Chengdu, 2016, pp. 8654-8659.

[24] S. Lyden and M. E. Haque, "A Simulated Annealing Global Maximum Power Point

Tracking Approach for PV Modules Under Partial Shading Conditions," in *IEEE Transactions on Power Electronics*, vol. 31, no. 6, pp. 4171-4181, June 2016.

[25] Y. Fan et al., "An improved simulated annealing maximum power point tracking technique for PV array under partial shading conditions," *18th European Conference on Power Electronics and Applications* (EPE'16 ECCE Europe), Karlsruhe, 2016, pp. 1-8.

[26] H. Renaudineau et al., "A PSO-Based Global MPPT Technique for Distributed PV Power Generation," in *IEEE Transactions on Industrial Electronics*, vol. 62, no. 2, pp. 1047-1058, Feb. 2015.

[27] G. Z ̈apfel, R. Braune, and M. B ̈ogl, *Metaheuristic Search Concepts*: A Tutorial with Applications to Production and Logistics. Dordrecht: Springer, 2010.

[28] D. L. Poole and[1-8] A. K. Mackworth, Artificial Intelligence: Foundations of Computational Agents. *Cambridge: Cambridge University Press,* 2010.

[29] K. Sundareswaran, V. V. Kumar, S. P. Simon , et al, "Cascaded simulated annealing/perturb and observe method for MPPT in PV systems," *IEEE International Conference on Power Electronics, Drives and Energy Systems* (PEDES), Trivandrum, 2016, pp. 1-5.

[30] S. Lyden and M. E. Haque, "A hybrid simulated annealing and perturb and observe method for maximum power point tracking in PV systems under partial shading conditions," *Australasian Universities Power Engineering Conference* (AUPEC), Wollongong, NSW, 2015, pp. 1-6.

[31] S. M. Mirhassani, M. Razzazan and A. Ramezani, "An improved PSO based MPPT approach to cope with partially shaded condition," *22nd Iranian Conference on Electrical Engineering* (ICEE), Tehran, 2014, pp. 550-555.

[32] H. Renaudineau et al., "A PSO-Based Global MPPT Technique for Distributed PV Power Generation," in *IEEE Transactions on Industrial Electronics*, vol. 62, no. 2, pp. 1047-1058, Feb. 2015.

[33] L. Du, D. Zhang, Z. Xu , et al, "Research on MPPT Algorithm Based on Variable-Step Conductance Increment Method and Pseudo-MPP Correction," *International Conference on Industrial Informatics - Computing Technology, Intelligent Technology, Industrial Information Integration* (ICIICII), Wuhan, China, 2017, pp. 342-345.

[34] J. Liu, J. Li, J. Wu and W. Zhou, "Global MPPT algorithm with coordinated control of PSO and INC for rooftop PV array," in *The Journal of Engineering*, vol. 2017, no. 13,

pp. 778-782, 2017.

[35] V. Phimmasone, Y. Kondo, N. Shiota , et al, "The effectiveness evaluation of the newly improved PSO-based MPPT controlling multiple PV arrays," *1st International Future Energy Electronics Conference* (IFEEC), Tainan, 2013, pp. 81-86.

[36] V. Phimmasone, Y. Kondo, N. Shiota, et al, "The demonstration experiments to verify the effectiveness of the improved PSO-based MPPT controlling multiple photovoltaic arrays," *IEEE ECCE Asia Downunder*, Melbourne, VIC, 2013, pp. 86-92.

[37] T. Guan and F. Zhuo, "An improved SA-PSO global maximum power point tracking method of photovoltaic system under partial shading conditions," *IEEE International Conference on Environment and Electrical Engineering and IEEE Industrial and Commercial Power Systems Europe* (EEEIC / I&CPS Europe), Milan, 2017, pp. 1-5.

[38] P. Li, N. Cui, Z. Kong and C. Zhang, "Energy management of a parallel plug-in hybrid electric vehicle based on SA-PSO algorithm," *36th Chinese Control Conference* (CCC), Dalian, 2017, pp. 9220-9225.

[39] Taher NIKNAM,Babak AMIRI,Javad OLAMAEI, et al.An efficient hybrid evolutionary optimization algorithm based on PSO and SA for clustering[J].*Journal of Zhejiang University*(Science A:An International Applied Physics & Engineering Journal),2009,10(04):512-519.

[40] S. Sudibyo, M. N. Murat and N. Aziz, "Simulated annealing-Particle Swarm Optimization (SA-PSO): Particle distribution study and application in Neural Wiener-based NMPC," *10th Asian Control Conference* (ASCC), Kota Kinabalu, 2015, pp. 1-6.

[41] K. L. Lian and V. Andrean, "A new MPPT method for partially shaded PV system by combining modified INC and simulated annealing algorithm," *International Conference on High Voltage Engineering and Power Systems* (ICHVEPS), Bali, 2017, pp. 388-393.

[42] K. Sundareswaran, V. V. Kumar, S. P. Simon , et al, "Cascaded simulated annealing/perturb and observe method for MPPT in PV systems," *IEEE International Conference on Power Electronics, Drives and Energy Systems* (PEDES), Trivandrum, 2016, pp. 1-5.

[43] M. De Cristofaro, G. Di Capua, N. Femia, et al , "Models and methods for energy productivity analysis of PV systems," *IEEE 13th International Conference on Industrial Informatics* (INDIN), Cambridge, 2015, pp. 1153-1158.